Breakdown of the Ostwald Step Rule--The Precipitation of Calcite and Dolomite from Seawater at 25 and 40^{o}C

by

Tingting Wang

A thesis submitted to McGill University in partial fulfilment of the
requirements of the degree of Master of Science

Earth and Planetary Sciences
McGill University
Montreal, Canada
July 2012

Contribution of Authors

I, hereby, declare that all the laboratory and analytical work presented in this thesis was completed by myself. The subject of this thesis was proposed by Professor Alfonso Mucci. Professor Alfonso Mucci provided guidance on the research methodology, advised me with the processing and interpretation of the data and contributed to the preparation of this thesis.

Acknowledgements

First and foremost, I would like to express my gratitude to my supervisor Dr. Alfonso Mucci. He provided me with a scientific environment where it was possible to learn and experience the rigour of science. I also want to thank him for his patience and encouragement from the inception of this thesis to its completion. His thoughtful comments and suggestions helped to shape this thesis. Without his guidance and support, I would not have been able to complete this project and thesis.

I would also like to thank my fiancé Xin Xu. Completion of this project and thesis would not have been possible without his encouragement, help and moral support. Many thanks for his patience and encouragement. I was fortunate enough to have him throughout this period my life. Thank you--my love--for the considerable time and effort put forth regarding my M.Sc. project.

I would like to thank Michel Preda, Constance Guignard, and Isabelle Richer, for their assistance with the geochemical and instrumental analyses. They provided valuable guidance and advice for the experimental section of this thesis.

I also wish to thank my parents to their unequivocal support throughout, as always, for which my mere expression of thanks likewise does not suffice.

I would like to thank my dear colleagues and friends: Thais Lamana, Qiang Chen, Stelly Lefort, Fatimah Sulu-Gambari, Adrian Villegas, Dominique Richard, Steve Pratte, Maryon Paulsen Strugstad, Liping Bai, Victoria Maneta, and Mohadeseh Majnoon for their help and advice.

Abstract

The scarcity of recent dolomite contrasts strongly with its common abundance in ancient sedimentary rocks, leading to the paradox commonly referred to as the "dolomite problem". Despite many attempts, dolomite has never been precipitated at room temperature from natural seawater in the absence of bacterial mediation. It has been proposed that natural environments conducive to dolomite formation may be dynamic systems, in which the water chemistry (pH, alkalinity, saturation state with respect to specific minerals) fluctuates in response to variations in environmental conditions such as biological activity, temperature, salinity. Nevertheless, there is little literature dedicated to simulating such environmental changes. In this study, we simulated the dynamic nature of natural environments by alternating between intervals of dissolution and precipitation in natural seawater through purging gases of different CO_2 partial pressures (pCO_2). By alternating between periods of aragonite supersaturation and undersaturation, aragonite was obtained during the first few cycles at 25 and 40^{o}C, but only calcite was detected in the 18th cycle of the experiments at 25^{o}C. In contrast, neither calcite nor dolomite were detected in the precipitates after 20 and 25 cycles at 40^{o}C. Parts of the objectives in this study—breaking the Ostwald Step Rule and synthesizing calcite from natural seawater at 25^{o}C—were achieved, but the 40^{o}C experiment did not yield the result we hoped for. One possible explanation is that stable calcite nuclei may not have accumulated to a high enough concentration after 25 cycles at 40^{o}C that sufficient calcite surfaces were available to offset the nucleation of aragonite. Another explanation is that stable pre-nucleation clusters,

whose conformation may also be dependent on solution composition and temperature, control the crystallization of a set calcium carbonate polymorph.

Résumé

La rareté de la dolomite récente contraste avec son abondance dans des roches sédimentaires anciennes, conduisant au paradoxe communément appelé "le problème de la dolomite". Malgré de nombreuses tentatives, en l'absence de médiation bactérienne, la dolomie n'a jamais été précipitée à la température ambiante à partir de l'eau de mer naturelle. Il a été proposé que les environnements naturels propices à la formation de dolomite peuvent être des systèmes dynamiques, pour lesquels la chimie de l'eau (pH, alcalinité, l'état de saturation à l'égard de minéraux spécifiques) fluctue en réponse aux variations des conditions environnementales (par ex.: l'activité biologique, la température, la salinité). Cependant, il y a très peu de la littérature consacrée à la simulation de ces changements environnementaux. Dans cette étude, nous avons simulé, en alternant entre des intervalles de dissolution et de précipitation dans l'eau de mer naturelle par une purge de gaz de différentes pressions partielles en CO_2 (pCO_2), la nature dynamique des milieux naturels. En alternant entre des périodes de sur-saturation et sous-saturation par rapport à l'aragonite, seule de la calcite a été détectée après le 18ième cycle à 25 °C. En revanche, nous n'avons observé ni calcite et ni dolomite dans les précipités aragonitiques après 20 et 25 cycles à 40 °C. Une partie des objectifs de cette étude - contrer règle d'Ostwald sur les transformations successives (états intermédaires) et la synthèse de calcite dans l'eau de mer naturelle à 25 °C - ont été atteints, mais l'expérience à 40^{o}C n'a pas donné le résultat espéré. Une explication possible est que des noyaux stables de calcite ne se sont pas accumulés à une concentration assez élevée après 25 cycles

à 40 °C, que suffisamment de surface calcitique était disponible pour contrer la nucléation de l'aragonite. Une autre explication est que la stabilité des grappes de pré-nucléation, dont la conformation dépend possiblement de la chimie de la solution et de la température, se forment et contrôlent la cristallisation d'un polymorphe spécifique de carbonate de calcium.

Table of Contents

List of Tables

List of Figures

Chapter 1 Introduction and Literature Review

1.1 Introduction

1.1.1 Occurrence of Carbonate Minerals and Their Stability

Under Earth surface conditions, carbonate minerals are among the most chemically reactive and ubiquitous minerals in both marine and fresh water environments (Morse et al., 2007). Calcite ($CaCO_3$(s)) and dolomite ($CaMg(CO_3)_2$(s)) are by far the most abundant rock-forming carbonate minerals, comprising more than 90% of natural carbonates in the Earth's crust (Reeder, 1983). In modern sediments, aragonite and high-magnesian calcites dominate in shallow-water environments, whereas low magnesium calcite (<4 mole% $MgCO_3$(s)) composes almost all deep-sea carbonate-rich sediments (Morse et al., 2007). These minerals largely impact the chemistry of aquatic systems by regulating pH and alkalinity through dissolution/precipitation equilibra, as well as their sorption capacity for divalent cations.

There are three polymorphs of anhydrous calcium carbonate: vaterite, aragonite, and calcite, listed here in order of increasing thermodynamic stability. The aragonite-calcite equilibrium phase diagram (Figure 1.1) shows that aragonite is the stable phase at high pressure and relatively low temperature in the Earth's crust. This stability field is consistent with the higher Ca coordination in aragonite (9-fold as opposed to 6-fold coordination to surrounding oxygen atoms in calcite) and its greater density. The metastability of aragonite in nature is demonstrated by its fairly common occurrence in high-pressure rocks which have been uplifted to the Earth's surface, as well as by its (biogenic and abiotic) formation and persistence in low-temperature sedimentary environments. The preservation of metastable aragonite in marine environments is frequently attributed to the presence of Mg^{2+} in solution which may inhibit calcite nucleation and the aragonite to calcite transformation (e.g. Bischoff, 1968; Davis et al., 2000, 2004; Yoshioka et al., 1986; Lin and Singer, 2009; Choudens-Sánchez and González, 2009). Under Earth surface conditions, the transformation of aragonite to calcite in aqueous solutions proceeds by a mechanism of dissolution and re-precipitation via the fluid phase (Fyfe and Bischoff, 1965). The textures of natural, partially-transformed aragonites show many small calcite crystals throughout the aragonite, suggesting that the slow growth rate of calcite rather than its nucleation rate is responsible for the preservation of aragonite during the phase transformation (Rehman et al., 1994).

Saturation conditions with respect to minerals may be expressed as the saturation state Ω,

$$\Omega = \frac{ICP}{K_{SP}^{*}} \tag{1}$$

where ICP is the ion concentration product and K_{SP}^{*} is the stoichiometric solubility product of the mineral. The latter is a function of the in situ temperature, pressure and salinity. For calcite, the saturation state, Ω_c, is expressed as:

$$\Omega_c = \frac{[Ca^{2+}]_{sw} * [CO_3^{2-}]_{sw}}{K_{SP}^{*}} \tag{2}$$

where $[Ca^{2+}]_{sw}$ and $[CO_3^{2-}]_{sw}$ are the concentrations of Ca^{2+} and CO_3^{2-} in seawater, respectively. When $\Omega_c < 1$, the solution is undersaturated with respect to calcite and, in the presence of solid calcite, dissolution should occur. When $\Omega_c = 1$, the system is at equilibrium. When $\Omega_c > 1$, the solution is supersaturated and precipitation of calcite should occur, provided seeds are present in the solution or the supersaturation is high enough to induce spontaneous nucleation. A similar scenario can apply to aragonite. Alternatively, the degree of saturation of a solution with respect to a mineral can also be characterized by the saturation index (SI). SI is the log of the saturation state Ω or:

$$SI = \log\Omega = \log\left(\frac{ICP}{K_{SP}^{*}}\right) \qquad (3)$$

Hence, at equilibrium, $SI = 0$.

1.1.2 The Dolomite Problem

Dolomite and the uncertainties regarding its origin have attracted the attention of earth scientists for over two centuries (de Dolomieu, 1791; Haidinger, 1845; Zenger et al., 1994). Dolomite was far more common than calcite in the Precambrian and it is thought that its relative abundance decreased from the Palaeozoic through the Mesozoic-Cenozoic (e.g., Chilingar, 1956; Ronov, 1964). The relative abundance of ancient dolomite has been reported to positively correlate with periods of high sea-level stand and warm climatic conditions during which calcitic ooids and cements are common (e.g., see discussions of Mackenzie and Morse, 1992; Arvidson and Mackenzie, 1996). Although surface seawater in today's oceans is highly supersaturated with respect to dolomite, there is no evidence of widespread dolomite precipitation in modern marine sediments. Modern dolomite, as a primary precipitate in nature, is only found in marginal hypersaline aquatic environments such as the Coorong Lakes of South Australia (Alderman, 1959; McKirdy et al., 2010), in deep-sea sediments (Lumsden, 1988) and in sediments of hypersaline lakes undergoing strong solar evaporation (Jones, 1961). Most dolomitic sediments are produced from the reaction of calcium carbonate deposits with magnesium-bearing solutions (Lippmann, 1973). These secondary dolomites are either formed from unconsolidated calcite sediments on the seafloor (Mitchell et al., 1987), or much later when magnesium-bearing solutions percolate calcium carbonate rocks through faults and joints at or near hydrothermal sources (Lovering, 1969; Ilich, 1974; Steefel and Van Cappellen, 1990).

Lippmann (1973, 1982) showed that seawater supersaturation with respect to dolomite can persist for centuries. The scarcity of recent dolomite contrasts strongly with its common abundance in ancient marine sedimentary rocks, leading to the paradox commonly referred to as the "dolomite problem". The fact that dolomite rarely precipitates out of modern seawater and $CaCO_3$ is seldom dolomitized on the seafloor is attributed to kinetic inhibition (Land 1998; Chai et al., 1995). The kinetic inhibition at low temperatures (below 100°C) results from the fast precipitation rate of metastable calcium carbonate minerals (e.g., vaterite, aragonite, calcite) and the strong hydration energy of the Mg^{2+} ion (Lippmann 1973, 1982; Folk and Land, 1975; Wright and Wacey, 2004). The formation of calcium carbonates is kinetically favoured because of their simpler structure (Folk and Land, 1975) and the lower free energy of hydration of the calcium ion (1579 kJ mole^{-1}) relative to the magnesium ion (1926 kJ mole^{-1}). Although seawater is supersaturated with respect to dolomite and the mineral should spontaneously precipitate, the carbonate ions cannot overcome the hydration shell of the Mg^{2+} ion to form a bond. After exposing calcite to a Mg-rich highly dolomite-supersaturated solution for 32 years in an attempt to precipitate dolomite at 25^{o}C, Land (1998) concluded: "...we all (?) now agree that 'The Dolomite Problem' is one of kinetics."

1.1.3 The Ostwald Step Rule

In 1897, Ostwald claimed as a universal principle, that a metastable solid phase will precipitate before the more stable phase if the solution is supersaturated with respect to the metastable phase (Nordeng and Sibley, 1994; Deelman, 1999, 2001). With the exception of the Arctic Ocean, surface seawater is supersaturated with respect to calcium and magnesium carbonate minerals (such as dolomite, calcite, aragonite, magnesite and high-magnesian calcite) (Lyakin, 1968). Dolomite can readily be precipitated from aqueous solutions above 100^{o}C (Arvidson and Mackenzie, 1999), but, without bacterial mediation (e.g. Vasconcelos and McKenzie, 1997; Kenward et al., 2009), most attempts to synthesize dolomite at room temperature from natural seawater have failed (e.g. Land 1985, 1998; Purser et al., 1994; McKenzie, 1991). Nevertheless, by alternating between intervals of dissolution and precipitation of a calcite-supersaturated artificial brine, Deelman (1999) succeeded in synthesizing dolomite at low temperatures (between 313K (40°C) and 333K (60°C)). He concluded that fluctuations in solution saturation, temperature or pressure can break the Ostwald Step Rule and provide conditions conducive to the low-temperature synthesis of dolomite. Deelman (1999) proposed that natural fluctuations in pH could result in alternating periods of dissolution and precipitation. During cycling of the solution between undersaturation and supersaturation with respect to metastable phases while remaining supersaturated with respect to more stable phases, metastable phases are leached, favouring the formation of the stable phases. Hence, according to Deelman (1999), dolomite can only be synthesized in dynamic systems in which environmental parameters are allowed to fluctuate, as is often the case in nature, but seldom applied in the laboratory. Fluctuating pH conditions are frequently observed in natural aquatic systems and occur at various frequencies (e.g. seasonal changes in water chemistry; daily changes caused by photosynthesis/respiration; temperature effect on gas solubility; evaporation; temporary isolation of a water body (e.g. lagoon); secular variations of atmospheric pCO_2, …)

1.2 Literature Review

1.2.1 Dolomitization Reactions

Dolomite is an unusual carbonate mineral. It is common in ancient platform carbonates, but is rare in Holocene sediments and, without bacterial mediation (Vasconcelos and McKenzie, 1997; Kenward et al., 2009), is difficult to precipitate in the laboratory at temperatures below 100^{o}C. Debate has raged for decades over whether dolomite is "primary" (i.e. precipitated directly from seawater) or "secondary" (post-depositional dolomitization of calcitic carbonates), and, if secondary, by what mechanism dolomitization occurs.

Direct dolomite precipitation can be described by the following reaction:

$$Ca^{2+} + Mg^{2+} + 2CO_3{}^{2-} = CaMg(CO_3)_2 \qquad (4)$$

Assuming that the activity of a pure solid phase is unity (Carpenter, 1980), the thermodynamic solubility product of dolomite, which equals to equilibrium ion activity product, can be expressed as:

$$K^o_{sp} = (Ca^{2+})(Mg^{2+})(CO_3{}^{2-})^2 \qquad (5)$$

Because of the difficulties in precipitating dolomite at low temperatures from aqueous solutions in the laboratory, the value of K^o_{sp} is not precisely known. The reported values of the solubility of dolomite at 25^{o}C and one atmosphere total pressure range from 10^{-17} to 10^{-19} (Kramer, 1959; Garrels et al., 1960; Hsu, 1963; Langmuir, 1971; Robie et al., 1979). All of the values were obtained from dissolving dolomite in aqueous solutions. Nevertheless, irrespective of the value (10^{-17} or 10^{-19}) used, calculations of the ion activity product ($10^{-15.01}$) show that seawater is supersaturated with respect to dolomite by at least two orders of magnitude (Lippmann, 1973). Therefore, based on free energy considerations (thermodynamics), reaction (4) should proceed to the right and dolomite should spontaneously precipitate from seawater; yet dolomite is a rare modern marine precipitate.

A similar argument can be made for dolomitization of a calcitic limestone by modern seawater where the reaction is described by (Hsu, 1967):

$$2CaCO_3 + Mg^{2+} = CaMg(CO_3)_2 + Ca^{2+} \tag{6}$$

The Gibbs free energy for this reaction, ΔG_n^o, is -7.66 kJ mole^{-1} for the aragonite to dolomite transformation and -5.77 kJ mole^{-1} for the calcite to dolomite transformation. The negative Gibbs free energies imply that the thermodynamic drive is towards dolomitization. Alternatively, the equilibrium constant for the reaction can be expressed as:

$$K^o_{(aragonite-dolomite)} = \frac{(Ca^{2+})}{(Mg^{2+})} = 1.49 \tag{7}$$

for the aragonite to dolomite transformation and,

$$K^o_{(calcite-dolomite)} = \frac{(Ca^{2+})}{(Mg^{2+})} = 1.08 \tag{8}$$

for the calcite to dolomite transformation.

In other words, the reactions should proceed to the right and aragonite and calcite should be dolomitized in solutions in which the $\frac{(Ca^{2+})}{(Mg^{2+})}$ is smaller than 1.49 and 1.08, respectively. As the Ca^{2+}:Mg^{2+} activity ratio of modern seawater is around 0.60, $CaCO_3$ should be dolomitized in seawater. Nevertheless, these reactions are not widespread.

An alternative version of reaction (6) was proposed by Lippmann (1973):

$$CaCO_3 + Mg^{2+} + CO_3^{2-} = CaMg(CO_3)_2 \tag{9}$$

wherein both Mg^{2+} and CO_3^{2-} ions are supplied by the dolomitizing fluid and all Ca^{2+} ions of the precursor $CaCO_3$ are incorporated into the dolomite. The Gibbs free energy of this reaction is -55.43 kJ mole^{-1} with aragonite as the precursor mineral and -54.47 kJ mole^{-1} with calcite as the precursor mineral, implying an even greater drive towards dolomitization.

Reactions (6) and (9) are most widely used to represent the formation of secondary dolomites, but both reactions are simplified and do not account for the porosity changes that accompany the conversion from $CaCO_3$ to dolomite. Because the molar volume of two moles of aragonite and calcite are 8% and 13% greater, respectively, than the molar volume of one mole of dolomite, reaction (6) explains why so many dolostones are more porous than calcitic limestones (Weyl, 1960; Michalowski and Asuero, 2012). Nevertheless, as clearly stated before (e.g. Chilingar and Terry, 1954; Bissel and Chilingar, 1958), this porosity generation will only occur if no additional dolomite is precipitated due to any external carbonate source, and if there is no subsequent compaction. Reaction (9), on the other hand, would involve a 75% or 88% increase in molar volume for aragonite or calcite replacement, respectively (Lippmann, 1973), and thus lead to considerable porosity loss during dolomitization. Hence, reaction (9) may be a more reasonable representation of dolomitization where dolomite occurs mainly as a cement. Many dolomitized platform carbonates display good to excellent fabric preservation with no porosity gain or loss (e.g. Halley and Schmoker, 1983; Lucia, 2004). For example, Halley and Schmoker (1983) confirmed that the porosity of many dolostones which have not been buried deeply, is similar to calcitic limestones. Clearly, neither reactions (6) nor (9) accounts for all natural dolomitization. This discussion suggests that natural replacement dolomitization may best be described by a combination of those two reactions, because it allows to adjust for preservation, gain, or loss of volume during the replacement process.

To circumvent this problem, Morrow (1982) combined reactions (6) and (9) as follows:

$$(2-x)CaCO_3 + Mg^{2+} + xCO_3{}^{2-} = CaMg(CO_3)_2 + (1-x)Ca^{2+} \qquad (10)$$

Reaction (10) is intermediate between reactions (6) and (9) (for x = 0, reactions (10) is equivalent to reaction (6), and for x = 1, reaction (10) becomes reaction (9)). When x is equal to “0.25” or “0.11”, representing, respectively, calcite and aragonite replacement, reaction (10) involves no volume gain or loss (Morrow, 1982) and represents cases of dolomitization with good fabric preservation. The Gibbs free energy of the aragonite to dolomite transformation reaction when x = 0.11 is -12.90 kJ mole^{-1} and -17.96 kJ mole^{-1} for the calcite to dolomite transformation when x = 0.25, as shown in Table 1.1.

1.2.2 The CaCO$_3$ (Calcite and Aragonite) Transformation to Dolomite and Dolomitization Models

The standard free energy of reaction (10) is:

$$\Delta G_r^o = RT \ln \frac{\dfrac{(Ca^{2+})^{1-x}}{Mg^{2+}(CO_3^{2-})^x}}{K} \qquad (11)$$

At equilibrium (ΔG_r^o is zero), the equation has three variables: temperature (T), the Ca^{2+}:Mg^{2+} activity ratio and Ca^{2+}:CO$_3^{2-}$ activity ratio. The calcite-dolomite field of stability boundary is therefore plotted versus these three variables (Figure 1.2; modified from Machel and Mountjoy, 1986). In this trivariate thermodynamic stability diagram, three processes would shift a solution into the dolomite field: a decrease in the Ca^{2+}:Mg^{2+} activity ratio, a decrease in the Ca^{2+}:CO_3^{2-} activity ratio and an increase in temperature.

Several broad categories of dolomitization model have been proposed for the interpretation of ancient dolomites, such as: the shallow-subtidal model (Holland and Zimmermann, 2000), the evaporative model (Laporte, 1967; Matter 1967), the meteoric-marine mixing-zone model (Warren, 2000; Back and Hanshaw, 1971), and the burial compaction model (Kohout, 1965). Of the above models for early dolomitization, the most widely cited model has been the meteoric-marine mixing-zone scenario. In this model, dilution of seawater by groundwater is thought to overcome the kinetic hindrances to dolomite precipitation (Figure 1.3; Land, 1973). As shown in Figure 1.3, whereas dolomite is supersaturated in solutions containing more than 5% seawater, calcite is undersaturated in a mixture of up to 50% seawater. Thus, in the interval between 5-50% seawater, the solution should be capable of dolomitization, unimpeded by calcite precipitation.

1.2.3 Aragonite to Calcite Transformation

At Earth surface temperatures and pressures, calcite is the stable $CaCO_3$ polymorph. Nevertheless, aragonite is a ubiquitous metastable polymorph, particularly in the marine environment. The kinetic and mechanisms of the aragonite to calcite transformation have been extensively investigated using various methods of characterization (Webb et al., 2009; Titschack et al., 2009; Parker et al., 2010).

The recrystallization of aragonite to calcite in aqueous solutions at 100^{o}C and lower temperatures was first reported more than 180 years ago following the experiments published by Rose (1837). This author found that aragonite, precipitated from aqueous solutions at 100^{o}C, must be filtered and dried immediately in order to avoid substantial admixtures of calcite. At 10^{o}C, aragonite immersed in pure water converts to calcite in the course of about a day (Fyfe and Bischoff, 1965). At room temperature, the time required for complete transformation is on the order of several months (Taft, 1967). The transformation of aragonite to calcite takes place through dissolution of the metastable phase and growth of the more stable calcite phase, as confirmed by the exchange of strontium as well as oxygen and carbon isotopes with fluids during the transformation (e.g., Allan and Matthews, 1982; Perdikouri et al., 2011; Titschack et al., 2009; McGregor and Gagan, 2003).

A series of kinetic experiments by Fyfe and Bischoff (1965), Bischoff and Fyfe (1968) and Bischoff (1969) demonstrated convincingly that any chemical species which favors aragonite precipitation also inhibits the aragonite-calcite transformation. In seawater, the retardation may be mainly caused by strong inhibitors, such as Mg^{2+} (Lin and Singer, 2009; Astilleros et al., 2010), but phosphate (So et al., 2011; Plant and House, 2002), sulfate (Bots et al., 2011), and many organic substances (Parsiegla and Katz, 2000; Manoli and Dalas, 2002; Lakshtanov et al., 2011) may also play a role. The special role of magnesium ion has been recognized since Leitmeier (1909) found that Mg^{2+} favored the precipitation of aragonite over calcite. It has been suggested that Mg^{2+} controls the polymorphic form of calcium carbonate in marine environments both in primary precipitation and in subsequent diagenetic aragonite-calcite transformations (Simkiss, 1964; Taft and Harbaugh, 1964; Rushdi, 1992). The inhibition mechanism of Mg^{2+} was ascribed to the inability of calcite nuclei to grow and the destabilization of the calcite crystal lattice when encumbered by adsorption of hydrated magnesium ions (Davis et al., 2000, 2004; Lin and Singer, 2009; Choudens-Sánchez and González, 2009). Given the Mg^{2+}:Ca^{2+} concentration ratio in modern seawater (5.2), the presence of Mg^{2+} accounts for the limited extent of aragonite to calcite transformation in seawater.

1.3 Research Objectives

Although it has been proposed that natural environments conducive to dolomite formation may be dynamic systems, in which water chemistry parameters (such as pH, alkalinity, saturation state with respect to specific mineral) are allowed to fluctuate, there is a scarcity of literature dedicated to simulating such environmental changes (Deelman, 1999, 2001; dos Anjos, 2011). In this study, through alternating between intervals of dissolution and precipitation in natural seawater by purging gases of different pCO_2, the dynamic nature of natural environments was simulated. The working hypothesis is that during multiple cycling of a solution between undersaturation and supersaturation with respect to metastable phases (i.e. amorphous calcium carbonate (ACC), vaterite, aragonite), the metastable phases are expected to dissolve, while preserving more stable nuclei (i.e. calcite and dolomite) in solution. Therefore, the objectives of this thesis are to break the Ostwald Step Rule and to synthesize calcite and dolomite from natural seawater at low temperatures (25 and $40^{o}C$).

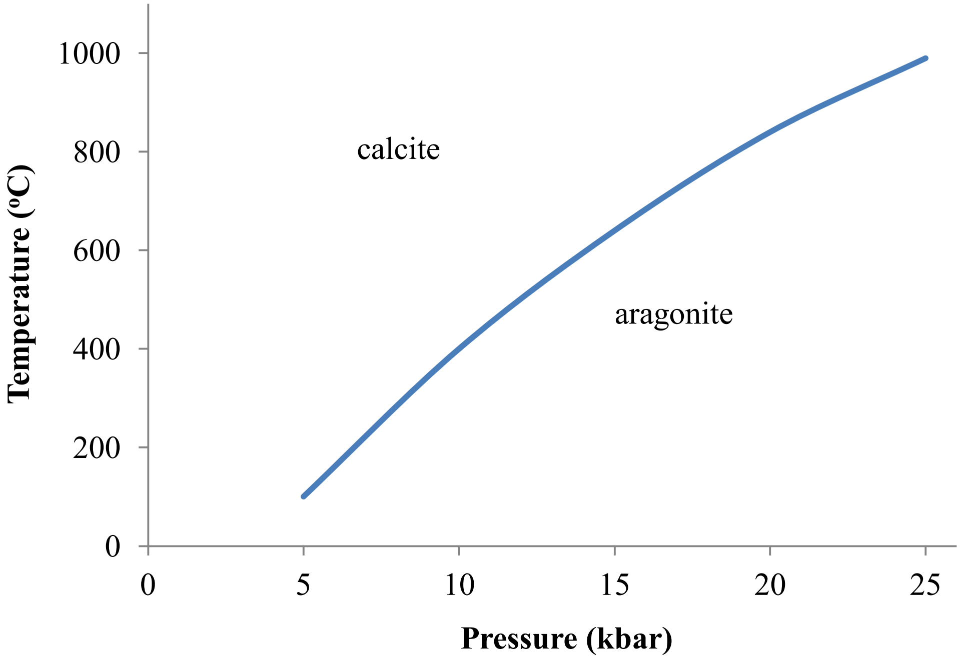

Figure 1.1 **The aragonite-calcite equilibrium phase diagram. Aragonite is stable at high pressures, while the stable polymorph under Earth surface conditions is calcite. (After Goldsmith and Newton, 1969).**

Table 1.1 Free energies of secondary dolomitization reactions with aragonite and calcite as starting materials: Reactions (6), (9) and (10)

	ΔG^o_r Aragonite (kJ/mole)	ΔG^o_r Calcite (kJ/mole)
$2CaCO_3 + Mg^{2+} = CaMg(CO_3)_2 + Ca^{2+}$	-7.66	-5.77
$CaCO_3 + Mg^{2+} + CO_3^{2-} = CaMg(CO_3)_2$	-55.43	-54.47
$(2-x)CaCO_3 + Mg^{2+} + xCO_3^{2-} = CaMg(CO_3)_2 + (1-x)Ca^{2+}$ (x = 0.11 for aragonite and x = 0.25 for calcite)	-12.90	-17.96

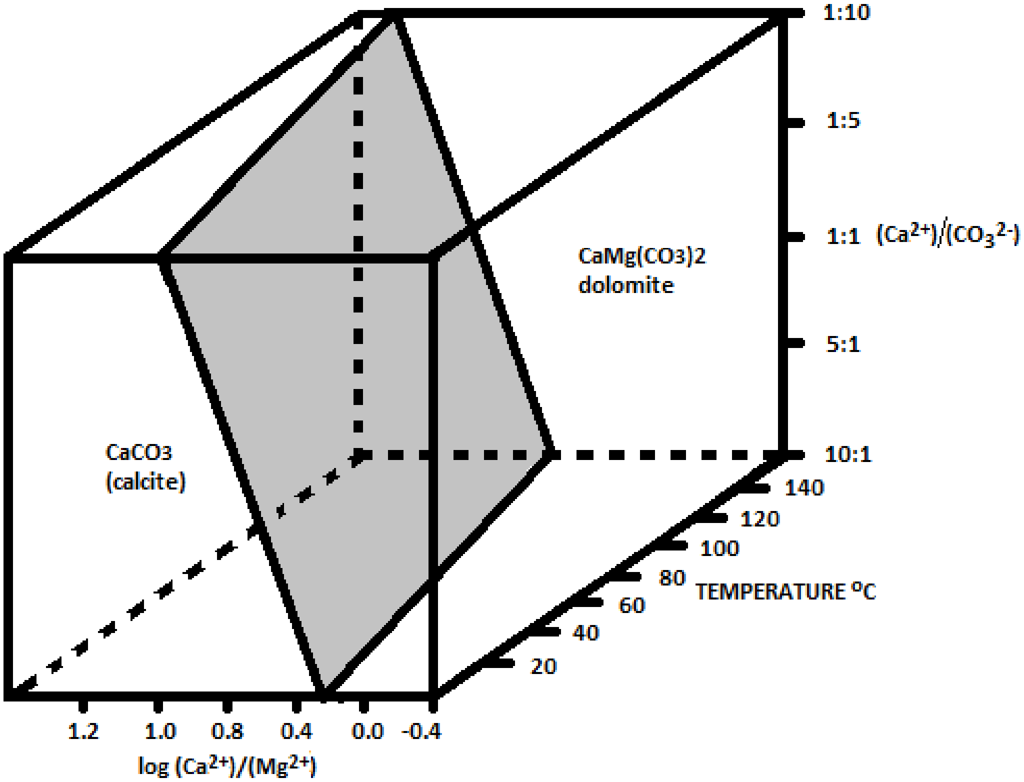

Figure 1.2 **Trivariate thermodynamic stability diagram for the system calcite-dolomite-water. The ionic ratios are activity ratios in the solution. The grey plane indicates the dividing boundary of the calcite-dolomite stability field, with dolomite to the right and calcite to the left. (reproduced from Machel and Mountjoy, 1986).**

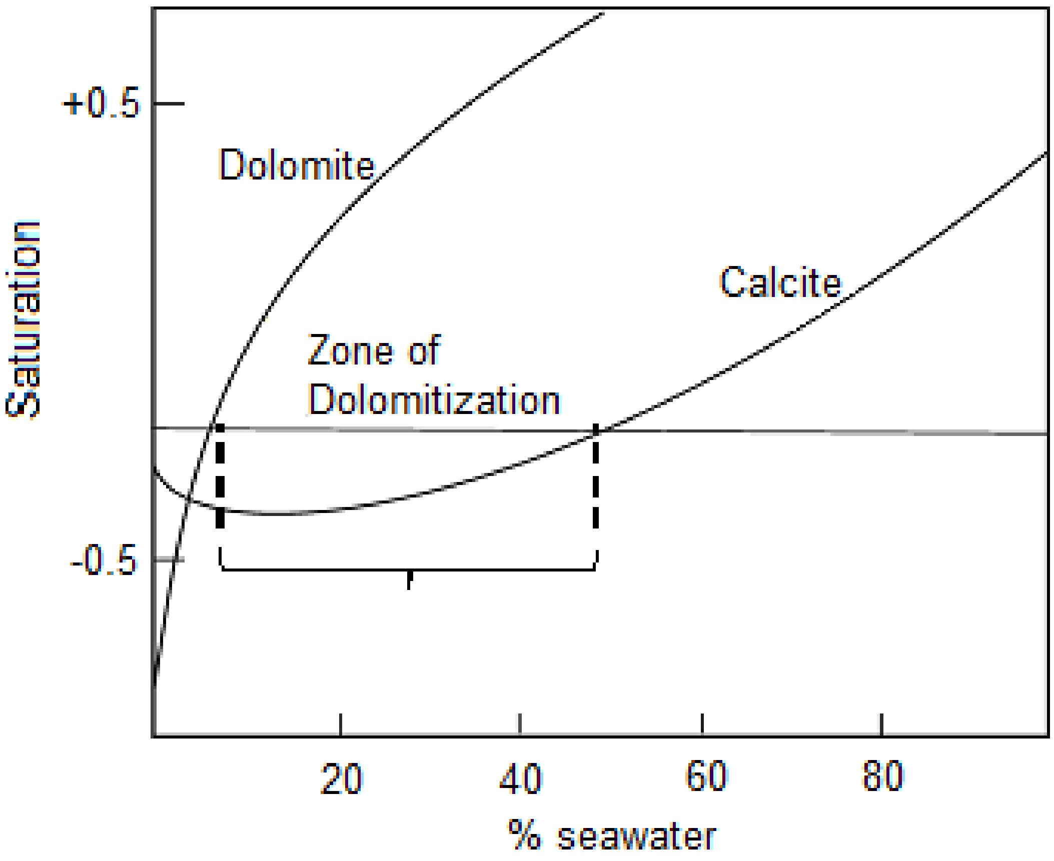

Figure 1.3 Meteoric-marine mixing-zone dolomitization model. The two curves show the saturation index of meteoric water with respect to dolomite and calcite as a function of seawater. Dolomitization is thought to take place in waters that are supersaturated with respect to dolomite but undersaturated with respect to calcite, identified as the *Zone of Dolomitization* in this figure. (reproduced from Hardie, 1987).

1.4 References

Alderman, A.R. (1959) Aspects of carbonate sedimentation. *J. Geol. Soc. Aust.* **6**, 1-10

Allan, J.R. and Matthews, R.K. (1982) Isotope signature associated with early meteoric diagenesis. *Sedimentology* **29**, 797-817

Arvidson, R.S. and Mackenzie, F.T. (1996) Tentative kinetic model for dolomite precipitation rate and its application to dolomite distribution. *Aquat. Geochem*. **2,** 273-298

Arvidson, R.S. and Mackenzie, F.T. (1999) The dolomite problem: control of precipitation kinetics by temperature and saturation state. *Am. J. Sci*. **299,** 257-288

Astilleros, J.M., Fernandez-Diaz, L. and Putnis, A. (2010) The role of magnesium in the growth of calcite: An AFM study. *Chem. Geol.* **271**, 52-58

Back, W. and Hanshaw, B.B. (1971) A geochemical hypothesis for dolomitization by ground water. *Econ. Geol.* **66**, 710-724

Bischoff, J.L. (1968) Kinetics of calcite nucleation: magnesium ion inhibition and ionic strength catalysis. *J. Geophys. Res*. **73**, 3315-3322

Bischoff, J.L. (1969) Temperature controls on aragonite-calcite transformation in aqueous solution. *Am. Mineral.* **54**, 149-155

Bischoff, J.L. and Fyfe, W.S. (1968) The aragonite-calcite transformation. *Am. J. Sci.* **266**, 65-79

Bissel, H.J. and Chilingar, G.V. (1958) Notes on diagenetic dolomitization. *J. Sediment. Petrol.* **28**, 490-497

Bots, P., Benning, L.G., Rickaby, R.E.M. and Shaw, S. (2011) The role of SO_4 in the switch from calcite to aragonite seas. *Geology* **39**, 331-334

Carpenter, A.B. (1980) The chemistry of dolomite formation I: the stability of dolomite. In: Concepts and Models of Dolomitization (Eds. D.H. Zenger, J.B. Dunham and R.L. Ethington), *Spec. Publ. Soc. Econ. Paleont. Miner.* **28**, 111-121.

Chai, L., Navrotsky, A. and Reeder, R.J. (1995) Energetics of calcium-rich dolomite. *Geochim. Cosmochim. Acta* **5**, 939-944

Chilingar, G.V. (1956) Relationship between Ca/Mg ratio and geological age. *Bull. Am. Ass. Petrol. Geol.* **40**, 2256-2266

Chilingar, G.V. and Terry, R.D. (1954) Relationship between porosity and chemical composition of carbonate rocks. *Petrol. Eng*. **26**, 341-343

Choudens-Sánchez, V.D. and González, L.A. (2009) Calcite and aragonite precipitation under controlled instantaneous supersaturation: Elucidating the role of $CaCO_3$ saturation state and Mg/Ca ratio on calcium carbonate polymorphism. *J. Sediment. Res*. **79**, 363-376

Davis, K.J., Dove, P.M. and De Yoreo, J.J. (2000) The role of Mg^{2+} as an impurity in calcite growth. *Science* **290**, 1134-1137

Davis, K.J., Dove, P.M., Wasylenski, L.E. and De Yoreo, J.J. (2004) Morphological consequences of differential Mg^{2+} incorporation at structurally distinct steps on calcite. *Am. Mineral*. **89**, 714-720

de Dolomieu, D. (1791) Sur un genre de pierres calcaires très peu effervescentes avec les acides et phosphorescentes par la collision. *J. Physique* **39**, 3-10

Deelman, J.C. (1999) Low-temperature nucleation of magnesite and dolomite. *N. Jb. Miner. Mh*. **7**, 289-302

Deelman, J.C. (2001) Breaking Ostwald's rule. *Chem. Erde* **61,** 224-235

dos Anjos, A.P.A., Sifeddine, A., Sanders, C.J. and Patchineelam, S.R. (2011) Synthesis of magnesite at low temperature. *Carbonates and Evaporites* **26**, 213-215

Folk, R.L. and Land, L.S. (1975) Mg/Ca ratio and salinity: two controls on crystallization of dolomite. *Am. Assoc. Petrol. Geol. Bull.* **59**, 60–68

Fyfe, W.S. and Bischoff, J.L. (1965) The calcite-aragonite problem. *Soc. Econ. Paleont. Mineral. Spec. Publ.* **13**, 3-13

Garrels, R.M., Thompson, M.E. and Siever, R. (1960) Stability of some carbonates at 25^oC and one atmosphere total pressure. *Am. J. Sci.* **258**, 402-418

Goldsmith, J.R. and Newton, R.C. (1969) P-T-X relations in the system $CaCO_3$-$MgCO_3$ at high temperatures and pressures. *Am. J. Sci.* **267-A**, 160-190

Haidinger, W. (1845) Ueber die Pseudomorphosen und ihre anogene und katogene Bildung. Abhandlungen der k. bohm. *Gesellschaft der Wissenschaften. Prague, Ser.5*. **3**, 231-259

Halley, R.B. and Schmoker, J.W. (1983) High-porosity Cenozoic carbonate rocks of southern Florida: progressive loss of porosity with depth. *Am. Assoc. Petrol. Geol. Bull*. **67**, 191-200

Hardie, L.A. (1987) Perspectives on dolomitization: A critical view of some current views. *J. Sediment. Petrol.* **57**, 166-183

Holland, H.D. and Zimmermann, H. (2000) The dolomite problem revisited. *Int. Geol. Rev.* **42**, 481–490

Hsu, K.J. (1963) Solubility of dolomite and composition of Florida ground waters. *J. Hydrol.* **1**, 288-310

Hsu, K.J. (1967) Chemistry of dolomite formation. In: Carbonate Rocks (Eds. G.V. Chilingar, H.J. Bissel and R.W. Fairbridge), Elsevier, Amsterdam, pp. 169-191.

Ilich, M. (1974) Hydrothermal-sedimentary dolomite: the missing link? *AAPG Bull.* **58**, 1331-1347

Jones, B.F. (1961) Zoning of saline minerals at Deeps Springs Lake, California. *Geol. Sci.* **421**, B199-B202

Kenward, P.A., Goldstein, R.H., Gonzalez, L.A. and Roberts, J.A. (2009) Precipitation of low-temperature dolomite from an anaerobic microbial consortium: the role of methanogenic *Archaea. Geobiology* **7**, 556-565

Kohout, F.A. (1965) A hypothesis concerning cyclic flow of salt water related to geothermal heating in the Florida aquifer. *N.Y. Acad. Sci.* **28**, 249–271

Kramer, J.R. (1959) Correction of some earlier data on calcite and dolomite in sea water. *J. Sediment. Petrol.* **29**, 465-467

Lakshtanov, L.Z., Bovet, N. and Stipp, S.L.S. (2011) Inhibition of calcite growth by alginate. *Geochim. Cosmochim. Acta* **75**, 3945-3955

Land, L.S. (1973) Contemporaneous dolomitization of middle Pleistocene reefs by meteoric water, north Jamaica. *Bull. Mar. Sci*. **23**, 64-92

Land, L.S. (1985) The origin of massive dolomite. *J. Geol. Educ.* **33**, 112-125

Land, L.S. (1998) Failure to precipitate dolomite at 25^{o}C from dilute solution despite 1000-fold oversaturation after 32 years. *Aquat. Geochem.* **4**, 361-368

Langmuir, D. (1971) The geochemistry of some carbonate ground waters in central Pennsylvania. *Geochim. Cosmochim. Acta* **35**, 1023-1045

Laporte, L.F. (1967) Carbonate deposition near mean sea-level and resultant facies mosaic: Manlius formation (lower Devonian) of New York State. *Am. Assoc. Petrol. Geol. Bull* **51**, 73-101

Leitmeier, H. (1909) Die absatze des mineralwasseus rohitsch-saverbrunn steiermark. *Z. Kryst.* **47**, 104

Lin, Y. and Singer, P.C. (2009) Effect of Mg^{2+} on the kinetics of calcite crystal growth. *J. Cryst. Growth* **312**, 136-140

Lippmann, F. (1973) Sedimentary Carbonate Minerals, Springer-Verlag, Berlin, pp. 228.

Lippmann, F. (1982) Stable and metastable solubility diagrams for the system $CaCO_3$-$MgCO_3$-H_2O at ordinary temperatures. *Bull. Mineral.* **105**, 273-279

Lovering, T.S. (1969) The origin of hydrothermal and low temperature dolomites. *Econ. Geol.* **64,** 743–754

Lucia, F.J. (2004) Origin and petrophysics of dolostone pore space. *J. Geol. Soc. London* **235**, 141-155

Lumsden, D.N. (1988) Characteristics of deep-marine dolomite. *J. Sediment. Res.* **58**, 1023-1031

Lyakin, Y.I. (1968) Calcium carbonate saturation of Pacific water. *Oceanology (USSR)* **8**, 44-53

Machel, H.G. and Mountjoy, E.W. (1986) Chemistry and environments of dolomitization--A reappraisal. *Earth-Sci. Rev.* **23**, 175-222

Matter, A. (1967) Tidal flat deposits in the Ordovician of Western Maryland. *Jour. Sed. Petrology* **37**, 601-609

Mackenzie, F.T. and Morse, J.W. (1992) Sedimentary carbonates through Phanerozoic time. *Geochim. Cosmochim. Acta* **56**, 3281-3295

Manoli, F. and Dalas, E.J. (2002) The effect of sodium alginate on the crystal growth of calcium carbonate. *Mater. Sci. Med.* **13**, 155-158

McGregor, H.V. and Gagan, M.K. (2003) Diagenesis and geochemistry of Porites corals from Papua New Guinea: implications for paleoclimate reconstruction. *Geochim. Cosmochim. Acta* **67**, 2147–2156

McKenzie, J.A. (1991) The dolomite problem: An outstanding controversy. In: Controversies in Modern Geology. (Eds. D.W. Muller), Academic Press, New York, pp. 490.

McKirdy, D.M., Hayball, A.J., Warren, J.K., Edwards, D. and Von der Borth, CH.C. (2010) Organic facies of Holocene carbonates in North Stromatolite

Lake, Coorong region, South Australia. *Xeoloxico de Laxe Coruna.* **35**, 127-146

Michalowski, T. and Asuero, A.G. (2012) Thermodynamic modelling of dolomite behavior in aqueous media. *J. Thermodyn*. **2012**, 1-12

Mitchell, J.T., Land, L.S. and Miser, D.E. (1987) Modern marine dolomite cement in a north Jamaican fringing reef. *Geology* **15**, 557-560

Morrow, D.W. (1982) Diagenesis I. Dolomite-part I: The chemistry of dolomitization and dolomite precipitation. *Geosci. Can*. **9**, 5-13

Morse, J.W., Arvidson, R.S. and Lüttge, A. (2007) Calcium carbonate formation and dissolution. *Chem. Rev*. **107**, 342-381

Nordeng, S.H. and Sibley, D.F. (1994) Dolomite stoichiometry and Ostwald's step rule. *Geochim. Cosmochim. Acta* **58**, 191-196

Parker, J.E., Thompson, S.P., Lennie, A.R., Potter, J. and Tang, C.C. (2010) A study of the aragonite-calcite transformation using Raman spectroscopy, synchrotron powder diffraction and scanning electron microscopy. *R. Soc. Chem.* **12**, 1590-1599

Parsiegla, K.I. and Katz, J.L. (2000) Calcite growth inhibition by copper (II) II. Effect of solution composition. *J. Cryst. Growth* **213**, 368–380

Perdikouri, C., Kasioptas, A., Geiser, T., Schmidt, B.C. and Putnis, A. (2011) Experimental study of the aragonite to calcite transition in aqueous solution. *Geochim. Cosmochim. Acta* **75**, 6211-6224

Plant, L.J. and House, W.A. (2002) Precipitation of calcite in the presence of inorganic phosphate. *Colloids Surf., A* **203**, 143–153

Purser, B.H., Tucker, M.E. and Zenger, D.H. (1994) Problems, progress and future research concerning dolomites and dolomitization. In: Dolomites: A Volume in Honour of Dolomieu (Eds. B.H. Purser, M.E. Tucker and D.H. Zenger), Blackwell Scientific Publications, Oxford, pp. 3–28.

Reeder, R.J. (1983) Crystal chemistry of the rhombohedral carbonates. *Rev. Mineral. Geochem.* **11**, 1-47

Rehman, J., Jones, B., Hagan, T.H. and Coniglio, M. (1994) The influence of sponge borings on aragonite-to-calcite inversion in late Pleistocene *strombus gigas* from Grand Cayman, British West Indies. *J. Sediment. Res.* **64**, 174-179

Robie, R.A., Hemingway, B.S. and Fisher, J.R. (1979) Thermodynamic Properties of Minerals and Related Substances at 298.15K and 1Bar (10^5 Pascals)

Pressure and at Higher Temperatures. *Geol. Survey Bull.* 1452. U.S. Gov. Printing Office, Washington, D.C., pp. 456.

Rose, G. (1837) Ueber die Bildung edes Kalkspaths and des Arragonits. *Poggendorfs Ann. Phys.* **42**, 353-367

Ronov, A.B. (1964) Common tendencies in the chemical evolution of the Earth's crust, ocean and atmosphere. *Geochem. Int*. **4**, 713-737

Rushdi, A.I. (1992) Mineralogy and morphology of calcium carbonate as a function of magnesium concentration in artificial seawater. *JKAU Mar. Sci.* **3**, 13–24

Simkiss, K. (1964) Variation in the crystalline form of calcium carbonate from artificial seawater. *Nature* **201**, 492-493

Steefel, C.I. and Van Cappellen, E. (1990) A new kinetic approach to modeling water-rock interaction: The role of nucleation, precursors, and Ostwald ripening. *Geochim Cosmochim Acta* **54**, 2657-2677

So, J.U., Postma, D., Jakobsen, R. and Larsen, F. (2011) Sorption of phosphate onto calcite; results from batch experiments and surface complexation modeling. *Geochim. Cosmochim. Acta* **75**, 2911-2923

Taft, W.H. (1967) Physical Chemistry of Formation of Carbonates. In: Carbonate Rocks (Eds. G.V. Chilingar; H.J. Bissell and R.W. Fairbridge), Elsevier, Amsterdam, pp. 151-168.

Taft, W.H. and Harbaugh, J.W. (1964) Modern Carbonate Sediments of Southern Florida, Bahamas and Espiritu Santo Island, Baja California: A Comparison of Their Mineralogy and Chemistry, *Stanford Univ. Publ. Geol. Sci*., **8***,* pp. 45-62.

Titschack, J., Radtke, U. and Freiwald, A. (2009) Dating and characterization of polymorphic transformation of aragonite to calcite in Pleistocene bivalves from Rhodes (Greece) by combined shell microstructure, stable isotope, and electron spin resonance study. *J. Sediment. Res*. **79**, 332-346

Vasconcelos, C. and McKenzie, J.A. (1997) Microbial mediation of modern dolomite precipitation and diagenesis under anoxic conditions (Lagoa Vermelha, Rio de Janeiro, Brazil). *J. Sediment. Res.* **67**, 378-390

Warren, J. (2000) Dolomite: occurrence, evolution and economically important associations. *Earth Sci. Rev.* **52**, 1–81

Webb, G.E., Northdurft, L.D., Kamber, B.S., Kloprogge, J.T. and Zhao, J.X. (2009) Rare earth element geochemistry of scleractinian coral skeleton during meteoric diagenesis: a sequence through neomorphism of aragonite to calcite. *Sedimentology* **56**, 1433-1463

Weyl, P. (1960) Porosity through dolomitization: conservation-of mass requirements. *J. Sediment. Petrol.* **30**, 85-90

Wright, D.T. and Wacey, D. (2004) Sedimentary dolomite – a reality check. In: The Geometry and Petrogenesis of Dolomite Hydrocarbon Reservoirs (Eds. C.J.R. Braithwaite, G. Rizzi and G. Darke). *The Geological Society London* **235**, pp. 65–74.

Yoshioka, S., Ohde, S., Kitano, Y. and Kanamori, N. (1986) Behaviour of magnesium and strontium during the transformation of coral aragonite to calcite in aquatic environments. *Mar. Chem.* **18**, 35-48

Zenger, D.H., Bourrouilh-Le Jan., F.G. and Carozzi, A.V. (1994) Dolomieu and the first description of dolomite. In: Dolomites: a Volume in Honour of Dolomieu (Eds. B.H. Purser, M. Tucker and D. Zenger), *Spec. Publ. Int. Assoc. Sedimentol.* **21**, 21-28

Chapter 2 Breakdown of the Ostwald Step Rule -- The Precipitation of Calcite and Dolomite from Seawater at 25 and 40^{o}C

Wang, T. and Mucci, A.

To be submitted to: Marine Chemistry

2.1 Abstract

The dynamic nature of some natural environments was simulated by alternating between periods of aragonite supersaturation and undersaturation in an attempt to nucleate calcite or dolomite from natural seawater. Aragonite was obtained during the first few cycles at 25 and 40^{o}C, but only calcite was detected in the 18th cycle of the experiments at 25^{o}C. In contrast, neither calcite nor dolomite were detected in the precipitates after 20 and 25 cycles at 40^{o}C. Hence, the Ostwald Step Rule was broken and calcite was precipitated from natural seawater at 25^{o}C under conditions that would normally yield aragonite.

2.2 Introduction

Carbonate minerals are common and important components of sediments and sedimentary rocks. Calcite ($CaCO_3(s)$) and dolomite ($CaMg(CO_3)_2(s)$) are by far the most abundant rock-forming carbonate minerals, comprising more than 90% of natural carbonates in the Earth's crust (Reeder, 1983). At Earth surface temperatures and pressures, calcite is the most stable polymorph of anhydrous calcium carbonate. The other two polymorphs are vaterite and aragonite, with the thermodynamic stability decreasing from calcite, aragonite to vaterite. Because of the importance of carbonates in the rock record, calcium carbonate precipitation and its transformation in aqueous solutions has received extensive consideration (e.g. Reddy and Wang, 1980; Morse and Mackenzie, 1990; Shiraki and Brantley, 1995; Kawano et al., 2009; Perdikouri et al., 2011). In many low temperature systems (below 100°C), polymorphic mineral precipitation in supersaturated parent solutions often occurs according the Ostwald Step Rule, which consists of a sequence of precipitation events where metastable solid phases nucleate first and are progressively replaced by more stable phases (Ostwald, 1897). Likewise, Nancollas (1982) and Nancollas et al. (1983) reported that mixed metastable mineral phases may arise in supersaturated solutions and are replaced by more stable phases through a series of dissolution–reprecipitation reactions, such as the polymorphic transformation of vaterite to calcite (Schmidt et al., 2010; Rodriguez-Blanco et al., 2011) and aragonite to calcite (Perdikouri et al., 2011; Titschack et al., 2009; McGregor and Gagan, 2003).

Dolomite is an unusual carbonate mineral. It is more common than calcite in Precambrian marine sediments and its relative abundance decreases from the Palaeozoic through the Mesozoic-Cenozoic (e.g., Vasconcelos et al., 1995; Chilingar, 1956; Ronov, 1964; Sanchez-Roman et al., 2008). Although surface seawater is more than 20 times supersaturated with respect to dolomite, there is little evidence of widespread dolomite precipitation in modern marine sediments. The scarcity of modern dolomite contrasts strongly with its common abundance in ancient marine sedimentary rocks, leading to the paradox commonly referred to as the "dolomite problem". Although dolomite can be readily precipitated in the laboratory from aqueous solutions above 100^{o}C (Arvidson and Mackenzie, 1999), without bacterial mediation (e.g. Vasconcelos and McKenzie, 1997; Kenward et al., 2009), most attempts to precipitate dolomite in the laboratory at low temperature (below 100^{o}C) from natural or synthetic seawater have failed (Land 1985, 1998; Purser et al., 1994; McKenzie, 1991). The paradox stems from dolomite's unique mineralogy and chemistry, and it is widely accepted that the most important factor controlling dolomite precipitation is kinetics (e.g. Land, 1985, 1998; Chai et al., 1995). It has been proposed that low-temperature dolomite formation may be microbially-mediated or promoted by the presence of organic compounds (i.e. extracellular polymeric substances, dissolved polysaccharides) (Kenward et al., 2009; Teng et al., 2012; Krause et al., 2012). Fluctuations in water chemistry or environmental variables, such as temperature, may also be conductive to dolomite formation (Oppenheimer and Master, 1965; Deelman, 1999). Hence, to date, the failure to precipitate dolomite at low temperature in the laboratory may due to the absence of a catalyst or suitable microbial community, or neglecting to simulate fluctuating chemical/ environmental conditions commonly encountered in natural settings.

Natural environments conductive to dolomite formation are believed to be dynamic, in which environmental parameters are allowed to fluctuate on various time scales (Deelman, 1999, 2001; dos Anjos et al., 2011). For instance, several parameters, such as temperature and its effect on gas solubility, temporary isolation of a water body, and secular variations of atmospheric pCO_2, will affect water chemistry including pH, alkalinity, saturation state with respect to specific minerals. Nevertheless, fluctuations of these parameters on dolomite precipitation, on the time scale of laboratory experiments, have seldom been investigated at low-temperature (Deelman, 1999, 2001). In this study, we simulated, in the laboratory, the dynamic nature of natural environments by alternatively bubbling gases of significantly different pCO_2 and alternating between intervals of aragonite dissolution and $CaCO_3$ precipitation in natural seawater.

2.3 Materials and Methods

2.3.1 Materials

All the laboratory glassware used throughout the experiments was acid-washed in a 10% HCl acid bath for a minimum of 24 hours, rinsed with distilled water several times and air-dried. The natural seawater was collected from 300 m depth in the Lower St. Lawrence Estuary in front of Rimouski, Quebec. It has a salinity of 34.5 and a total alkalinity of 2290 µmol/kg-SW. The reagent grade $CaCO_3$ powder used as starting mineral (preparation of the $CaCO_3$-saturated experimental solution) was purchased from Alfa Aesar, and an XRD analysis revealed that, based on our aragonite-calcite calibration curve (refer to sub-section 2.3.3 for details), it was composed of a mixture of 56% aragonite and 44% calcite. All the instrumental-grade CO_2/N_2 gas mixtures (with nominal pCO_2 of 50000 ppm or 100000 ppm) were purchased from Praxair Inc. Ontario, and the accuracy of the mixture composition was ±0.02%, as verified from the calculated pCO_2

value obtained from pH and alkalinity measurements on solutions equilibrated with the gases and calculated using the CO2SYS algorithm (refer to sub-section 2.3.5 for details).

2.3.2 Laboratory Experiments

The initial experimental solutions were prepared by equilibrating 2 L of natural seawater with 5 g of reagent grade $CaCO_3$ in a 2 L glass Erlenmeyer flask while bubbling, through a glass frit held near the bottom of the flask, a commercial CO_2/N_2 gas mixture at a nominal pCO_2 of 5% or 50000 ppm at constant rate at 0.5 ml/sec. At $25^{o}C$, the seawater solution was equilibrated with the gas for 3-4 hours or until the solution pH(TRIS) reached a steady-state value of ~6.73. After reaching this value, the solution was vacuum-filtered through a 0.45 μm Millipore HA filter to remove the $CaCO_3$ solid. Two aliquots of the filtered solution (50 mL) were taken, one for immediate (within 24 hours) titration of its total alkalinity and chlorinity and the other was acidified with a 1% equivalent volume of concentrated HNO_3 before being stored at $4^{o}C$ for later Ca and Mg analyses. Ambient laboratory air ($pCO_2 = 10^{-3.42}$ or ~390ppm) was bubbled at a constant rate of ~1.5 ml/sec through the CO_2-charged $CaCO_3$-equilibrated seawater solution until nucleation and precipitation of $CaCO_3$ was observed at the bottom of the flask, typically after 1-1.5 days. The solids were then vacuum-filtered through a 0.45 μm Millipore HA filter, rinsed with ~25 mL of Milli-Q water and methanol to remove residual seawater salts, air dried and stored in glass vials for later determination of their mineralogy by X-ray diffraction spectrometry. Two aliquots of the filtered solution were also taken, as described previously, for total alkalinity, chlorinity, Ca and Mg analyses, results of which were used for mass balance calculations. The protocol described above was repeated three times to confirm that the same precipitate mineralogy was obtained.

In subsequent experiments, the initial solution was prepared as described above, but the original (first cycle) precipitate was not filtered out and allowed to dissolve upon bubbling with a 10% (10000 pppm) CO_2/N_2 gas mixture. Once the solution pH(TRIS) reached a value of ~6.50, typically after 4 to 5 hours, and most of the precipitate was dissolved, ambient air was reintroduced to the solution. This cycle was repeated 17 times. As the number of cycles increased, precipitation of a solid required longer induction periods. On the 18th cycle, ultrapure N_2, instead of ambient laboratory air, was bubbled through the CO_2-charged seawater solution to further lower the pCO_2 and maximize precipitate recovery. The precipitate present in solution after the last cycle was separated by vacuum filtration through a 0.45 μm Millipore HA membrane, rinsed with ~25 ml of Milli-Q water and methanol to remove residual seawater salts, air dried and stored in glass vials. The mineralogy of the solid was determined by X-ray powder diffraction. As described earlier, two aliquots of the final filtered solution were taken for total alkalinity, chlorinity/salinity, Ca and Mg analyses. Throughout all experiments, the salinity of the experimental solutions was monitored using a hand-held refractometer calibrated with IAPSO standard seawater and salinity adjusted to ±0.5 by dropwise additions of distilled water to compensate for evaporation.

Likewise, chlorinity titrations at each cycle served to confirm that salinity did not vary significantly during the experiments. Results of the chlorinity titrations indicate that throughout the experiments, the salinity was maintained at 34.5±0.6 (Figure 2.1). An additional 10-cycle experiment was carried out at 25°C using the same protocol.

At 40°C, one-cycle, 20-cycle and 25-cycle experiments were carried in a thermostated water bath using the same protocol described above at 25°C. Calculated target pH(TRIS) values and nucleation induction periods were slightly different than at 25°C. Details appear in the results section.

2.3.3 Aragonite-Calcite X-Ray Powder Diffraction Calibration Curve

An X-ray powder diffraction (XRD) calibration curve was constructed using a series of calcite-aragonite mixtures, ranging from 0 to 100 mole or wt.%, in 10% increments. The solid mixtures were prepared by weight using Baker® "Instra-analyzed flux reagent" grade calcite and laboratory synthesized aragonite. The mineralogy of the Baker® "Instra-analyzed flux reagent" grade calcite was confirmed by XRD to be pure calcite. Aragonite was synthesized in the laboratory by the method of Wray and Daniels (1957) as modified by Katz et al. (1972) at a temperature of 70°C. An X-ray diffraction analysis of this material indicates that both vaterite and calcite are below the detection limit whereas an SEM examination did not detect any vaterite and traces of calcite (estimated at less than 2%).

X-ray powder diffraction (XRD) analyses were carried out with a Siemens® model D-500 X-ray diffractometer using Cu-Kα radiation (40 kV and 30 mA) at a scanning speed of 0.00828° 2θ s^{-1}. The time constant was set at 2 s and the diffraction spectra was recorded using a proportional counter detector. The detection limits for calcite, aragonite and vaterite were 4, 5 and 9 mole%, respectively. The experimental data, the ratio of the main diffraction peak intensities of calcite (*hkl* = 104, 2θ = 34.32) and aragonite (*hkl* = 111, 2θ = 30.72°) as a function of the mole (or weight) fraction of the mixture, were fitted to a linear least-squares equation as shown in Figure 2.2.

Assuming that the specimen is a uniform mixture of two component solids, the calibration line can be described by the following equation:

$$I_C/I_A = 3.034 * X_C/X_A$$

where I_C/I_A represents the ratio of the intensities of the primary calcite and aragonite diffraction peaks in the mixture, and X_C/X_A is the mole fraction of calcite and aragonite in the mixed sample. The correlation coefficient, R^2, of the fit was 0.9944. Our results are in reasonably good agreement with the calibration curves and best linear least-squares fits of Kontoyannis and Vagenas (2000) and Dickinson and McGrath (2001) (Figure 2.2).

2.3.4 Analytical Methods

2.3.4.1 pH Measurements

pH measurements of the seawater solutions were carried out at regular intervals throughout the CO_2/N_2 and ambient-air bubbling cycles using a combination glass-reference electrode (Radiometer® GK2401C) connected to a Radiometer® M84 pH/millivolt-meter. The pH electrode was calibrated with a set of three NIST-traceable buffers (4.00, 7.00 and 10.00 at 25°C and 4.03, 6.97 and 9.88 at 40°C) as well as a TRIS (Tris (hydroxymeththyl) aminomethane) seawater buffer solution (8.074 at 25°C and 7.616 at 40°C, S = 35; Millero *et al.*, 1993). The pH values reported below are all on the seawater scale pH(TRIS). Measurements were made on the millivolt scale, the pH(NIST) was calculated using the Nernstian slope and E_0 obtained from the least-squares fit to the NIST-traceable buffers, and converted to pH(TRIS) using the offset value obtained from the TRIS buffer measurement. The correlation coefficient of the fit was always better than 0.9999. The reproducibility of the pH calibrations carried out before and after measurements of a single sample solution was better than ±0.005 pH units. Saturation state calculations using pH measurements performed on both scales (i.e. NIST and TRIS) and appropriate constants using CO2SYS agreed to within ±5% or better.

2.3.4.2 Total Alkalinity Titrations

The total alkalinity of the experimental solutions was determined by potentiometric titration of a known weight of the samples using an automated Radiometer (TitraLab865®) titrator, a Red Rod® combination pH electrode (pHC2001) and a dilute HCl solution (0.003N). The HCl solution was calibrated at the beginning and end of each titration session against a solution of known alkalinity, gravimetrically prepared using dried Na_2CO_3 standard, as well as certified Dickson seawater (CRM Batch #94). The reproducibility of the measurements was better than 0.5%.

2.3.4.3 Chlorinity (Salinity) Titrations

Chlorinity was determined by potentiometric titrations using an automated Radiometer (TTT80) titrator, a silver electrode, and a mercuric sulfate reference electrode. The $AgNO_3$ solution titrant was calibrated with IAPSO standard seawater (P140). The reproducibility of these measurements was better than ±1%.

2.3.4.4 Atomic Absorption Spectrophotometry

Dissolved Ca^{2+} and Mg^{2+} concentrations in the seawater samples (initial, intermediate and final solutions) were determined by atomic absorption spectrophotometry (Perkin-Elmer® AAnalyst-100) with an air-acetylene flame and an impact-bead burner, following dilutions (100-fold for Ca and 5000-fold for Mg) in 1% HNO_3. External aqueous AAS standards were prepared by appropriate dilution of 1000 ppm certified standard solutions (Plasmacal, ICP-AES and ICP-MS standard, NIST-traceable in 4% HNO_3) in 1% HNO_3. The precision of these analyses is estimated to be better than ±5% for both Ca and Mg. The detection limits for the Ca and Mg analyses are 2.0 µM and 0.5 µM, respectively.

2.3.4.5 Temperature Control of the Experiments

The 25°C experiments were carried out at room temperature, which was recorded to be 22.8±0.2°C. The difference between pH values at room temperature and 25°C is within 0.005°C, thus the difference in temperature has a negligible effect on the solution pH. Therefore, experiments carried out at room temperature were treated as if they were conducted at 25°C. The 2 L glass Erlenmeyer flasks used in the 40°C experiment were submerged in a thermostated water bath maintained to within ±0.1°C of the set temperature.

2.3.5 CO2SYS

The Windows version of CO2SYS, developed by E. Lewis and D. Wallace, was used to simulate changes in seawater chemistry and estimate the carbonate ion concentration from pH and alkalinity measurements in the experimental solutions. All calculations were carried out on the seawater pH scale, in order to estimate other parameters (such as saturation state with respect to aragonite and calcite) of seawater. Calcium concentration was measured directly by atomic absorption spectrophotometry, as described in sub-section 2.3.4.4. The soluble reactive phosphate and silicate concentrations in the seawater solutions after nearly two years of storage at room temperature in polyethylene carboys was 0.24 μmol/kg-SW and 11.8 μmol/kg-SW, respectively (M. Strugstad, pers. comm.). These values were determined spectrophotometrically by the phosphomolybdate blue and the yellow silicomolybdic acid methods, respectively (Murphy and Riley, 1962; Grasshoff, 1964). They were used as input parameters in CO2SYS, even though their impact on the results of the calculations is negligible.

2.4 Results

2.4.1 Saturation State Calculations of the Experimental Solutions with Respect to Calcite and Aragonite

Although the saturation state of the experimental solutions can be calculated using CO2SYS from the pCO_2 of the gas mixtures or ambient-air and assuming equilibrium with respect to a given solid phase (calcite, aragonite or dolomite), conservative methods of calculations were still applied to verify the results. The saturation state of a seawater solution with respect to calcite (or aragonite) can be expressed as:

$$\Omega = \frac{\left[Ca^{2+}\right]_{SW} \times \left[CO_3^{2-}\right]_{SW}}{K^*_{spc}} \tag{1}$$

where $\left[Ca^{2+}\right]_{SW}$ and $\left[CO_3^{2-}\right]_{SW}$ are the calcium and carbonate ion concentrations in seawater, respectively, and K^*_{spc} is the stoichiometric solubility constant of calcite (and K^*_{spa} for aragonite) at the temperature and salinity of interest. The calcium concentration was measured by atomic absorption spectrophotometry of filtered samples, and the seawater carbonate ion concentration was computed with CO2SYS using the measured salinity, pH(TRIS) and total alkalinity as input parameters. The K^*_{spc} and K^*_{spa} values determined by Mucci (1983) in seawater as a function of salinity and temperature were used for the calculations. At $S = 34.5$,

K^*_{spc} is equal to 4.30*10^{-7} mol^2/kg^2 at 25°C and 4.11*10^{-7} mol^2/kg^2 at 40°C, whereas K^*_{spa} is equal to 6.65*10^{-7} mol^2/kg^2 at 25°C and 5.90*10^{-7} mol^2/kg^2 at 40°C.

Three independent experiments were carried out at each temperature to verify the reproducibility of our observations. The raw data for each of the three experiments at both 25 and 40°C are summarized in Table 2.1 and Table 2.2 and the solution saturation state with respect to calcite, aragonite and dolomite at both temperatures are shown in Figure 2.3 and Figure 2.4. The minima of each curve in this figure were obtained during CO_2/N_2 bubbling (5% CO_2/N_2 for first cycle, and 10% for all other cycles), and the maxima were obtained during ambient laboratory-air bubbling. The solutions were in equilibrium (Ω_a =1) with respect to aragonite and slightly supersaturated (Ω_c >1) with respect to calcite during the 1st cycle of 5% CO_2/N_2 bubbling. During ambient-air bubbling, the saturation state with respect to calcite and aragonite rose rapidly until a precipitate was formed. The following cycles displayed similar patterns except that the solution was undersaturated with respect to aragonite and in equilibrium with calcite during 10% CO_2/N_2 bubbling. Saturation state calculations indicated that the solutions were alternatively undersaturated and supersaturated with respect to aragonite and in equilibrium and supersaturated with respect to calcite when the two different gas mixtures (5-10% CO_2/N_2 or ambient air) were bubbled through the solutions.

2.4.2 Saturation State Calculation of the Experimental Solutions with Respect to Dolomite and Selection of Constants

The saturation state of the experimental solutions with respect dolomite (Ω_d) can be calculated by:

$$\Omega_d = \frac{\left[Ca^{2+}\right]_{SW} \times \left[Mg^{2+}\right]_{SW} \times \left[CO_3^{2-}\right]_{SW}^2}{K_{spd}^*} \tag{2}$$

where $\left[Ca^{2+}\right]_{SW}$ and $\left[Mg^{2+}\right]_{SW}$ were measured directly by AAS and $\left[CO_3^{2-}\right]_{SW}$ was determined from CO2SYS using the measured salinity, pH and total alkalinity as input parameters. K_{spd}^* is the stoichiometric solubility constant of dolomite in seawater at the temperature and salinity of interest. The K_{sp}^* was calculated from K_{sp}^o (thermodynamic solubility constant) according to:

$$K_{sp}^* = \frac{K_{sp}^o}{\gamma Ca^{2+} \times \gamma Mg^{2+} \times \gamma\left(CO_3^{2-}\right)^2} \tag{3}$$

where γ (i), the total ion activity coefficients of Ca^{2+}, Mg^{2+} and CO_3^{2-} in each solution were estimated using the ion-pairing model of Millero and Pierrot (1998). The total ion activity coefficients in seawater (S = 34.5) and a temperature of 25°C and 40°C are presented in Table 2.3. Given the difficulties of synthesizing dolomite at low temperature (below 100°C), a broad range of thermodynamic solubility constant (K_{sp}^o) values at 25°C, ranging from $10^{-17.09}$ (Robie et al., 1979) to 10^{-19} (Garrels et al., 1960), can be found in the literature. The most commonly used value is $10^{-17.09}$ (Robie et al., 1979), a value derived from calorimetric measurements during the dissolution of dolomite in HCl at 27°C (Hemingway and

Robie, 1994). This value was used in our study to calculate K_{sp}^{*} ($10^{-12.77}$ mol^4/kg^4) and the saturation state of the experimental solutions with respect to dolomite at 25°C. At 40°C, the thermodynamic solubility constant (K_{sp}^{o}) was calculated using the Van Hoff's equation, assuming that the enthalpy of reaction is constant over the temperature range of interest (i.e., 25 to 40°C). Accordingly, the calculated K_{sp}^{o} value is $10^{-17.45}$ and K_{sp}^{*} is calculated to be $10^{-13.13}$ mol^4/kg^4 using equation (3). The latter value was used to calculate the saturation state of the experimental solutions with respect to dolomite at 40°C. As shown in Figure 2.4, unlike the pattern for calcite and aragonite, the experimental solutions always remain supersaturated ($\Omega_d > 1$) with respect to dolomite at 25 and 40°C during CO_2/N_2 and ambient-air bubbling.

2.4.3 The Mineralogy of the Precipitates at 25°C

Presumably, once each solution reached a constant pH value, a steady state had been achieved after each purging step. During the initial $CaCO_3$ saturation of the seawater solutions with the 5% CO_2/N_2 gas mixture at 25°C, the pH decreased rapidly, then gradually increased and reached the steady-state value of approximately 6.73 after 3-4 hours. After filtration, ambient laboratory air was bubbled through the CO_2-charged $CaCO_3$-equilibrated seawater solution until nucleation and precipitation of $CaCO_3$ was observed at the bottom of the flask, typically after 1-1.5 days. According to the XRD analysis of the 1st-cycle precipitates (Figure 2.5), aragonite was the only mineral present.

After preparing three new $CaCO_3$-saturated seawater solutions, the multi-cycle experiments were initiated leaving the first-cycle precipitate (presumably aragonite) in suspension. A similar pattern was observed during purging with the 10% CO_2/N_2 gas mixture, except that the steady-state pH dropped to around 6.50. In general, the steady state for the CO_2/N_2 purging step and the apparent dissolution of the solids were achieved within 1-1.5 days. When ambient air was bubbled into the homogeneous solution in the 18-cycle experiment, the solution pH increased dramatically, and gradually dropped before pH reached a steady-state value of approximately 7.96. In general, the steady state was achieved within 1-2 days for the 18-cycle experiments. On the other hand, a longer period (approximately 9 to 11 days) was required to observe nucleation and precipitation (see discussion in section 2.5.2). Due to the relatively low efficiency of the experiments and limited amount of solid precipitated, a total of 18 cycles, instead of 20 cycles as originally designed, were performed at 25°C. After the 18th cycle, the XRD analysis revealed that calcite was the only precipitate (Figure 2.6). Due to the limited amount (just visible) of precipitate, only the major peak of calcite ($2\theta = 34.32$) was detected and we could not readily determine its magnesium content. In an attempt to determine after which cycle the mineralogy of the precipitate changed, one additional 10-cycle experiment was performed, and the XRD analysis of this precipitate revealed that it was composed of pure aragonite (Figure 2.7).

2.4.4 The Mineralogy of the Precipitates at 40^oC

During the three parallel one-cycle experiments at 40^{o}C, solution pH varied in a pattern similar to those of the experiments carried out at 25°C, except that the steady-state pH(TRIS) at saturation was 6.62. Likewise, nucleation and precipitation of $CaCO_3$ was observed at the bottom of the flask after ~1 day ambient-air bubbling and the precipitates formed after the 1st cycle were solely aragonite (Figure 2.8).

In subsequent multi-cycle experiments, when the 10% CO_2/N_2 gas mixture was purged through the seawater solutions, the steady-state pH(TRIS) was approximately 6.38. The time required to reach a steady state at 40^{o}C was slightly shorter (<1 day) than at 25^{o}C due to the faster (gas exchange and dissolution) kinetics at higher temperature (Arrhenius, 1889). Like the 25°C experiments, a steady-state pH(TRIS) (7.95) was achieved within ~1 day of bubbling ambient air through the CO_2-charged seawater solution, but only 6 to 7 days were required before nucleation and precipitation could be observed. In contrast to the 25^{o}C experiments, after 20 cycles, the mineralogy of the precipitates did not change and remained aragonite (Figure 2.9). In an attempt to extend the experiments through more cycles, an additional 5 cycles were carried out after returning the 20-cycle precipitates to a supersaturated seawater solution, but the XRD analysis showed that the mineralogy of the precipitate remained the same after the 25th cycle (Figure 2.10).

2.5 Discussion

2.5.1 Calcium Carbonate Polymorph Precipitated from Natural Seawater and Breaking the Ostwald Step Rule

There are three polymorphs of anhydrous calcium carbonate: calcite, aragonite and vaterite. Although calcite is the most stable calcium carbonate phase at atmospheric temperature and pressure, the polymorph that precipitates and persists in warm and shallow marine environments is aragonite (Rao, 1990; James and Clarke, 1997; Morse et al., 2007).

In this study, aragonite was precipitated at both 25 and 40^{o}C in the one-cycle experiments. These results are consistent with natural observations and previous experimental results: aragonite is known to be the sole precipitate during homogeneous precipitation of calcium carbonate from supersaturated, natural or artificial seawater (e.g. Rushdi et al., 1992; Morse and He, 1993; Pokrovsky and Savenko, 1995; Morse et al., 1997; Waly et al., 2012). The presence of magnesium, one of the major ions in seawater, is believed to hinder calcite nucleation and growth as well as transformation of the metastable phase aragonite to calcite (Morse et al., 1997; Zhang and Dawe, 2000; Zhang et al., 2001; Lin and Singer, 2009). The precipitation of aragonite rather than calcite in the one-cycle experiment is directly attributable to the $[Mg^{2+}]:[Ca^{2+}]$ ratio, temperature and saturation state in the seawater solution. Previous studies indicated that at low $[Mg^{2+}]:[Ca^{2+}]$ ratios (~1), calcite is the dominant mineral phase, whereas high $[Mg^{2+}]:[Ca^{2+}]$ ratios favor the formation of aragonite (Kitano et al., 1962; Berner, 1975; Morse and He, 1993; Morse et al., 1997; Choudens-Sánchez and González, 2009). Since the $[Mg^{2+}]:[Ca^{2+}]$ ratio in normal seawater is 5.2 (Millero, 1996) (Table 2.1 and Table 2.2), aragonite is expected to be the dominant phase in the one-cycle experiments (Morse et al., 1997).

Many mechanisms have been proposed to explain the effect of Mg^{2+} on the kinetics of calcite nucleation and growth (Akin and Lagerwerff, 1965; Reddy and Wang, 1980; Mucci and Morse, 1983; Zhang and Dawe, 2000; Lopez et al., 2009). The two most common explanations are detailed below. One explanation is that Mg^{2+} can be incorporated into the calcite structure but not into the aragonite structure during nucleation and growth, increasing the solubility of the calcite (Berner, 1975; Reddy and Wang, 1980; Davis et al., 2004; Choudens-Sánchez and González, 2009). The cation site in rhombohedral calcite is smaller than in orthorhombic aragonite, and accordingly, the calcite structure can accommodate the smaller Mg^{2+} ions (the ionic radii for Mg^{2+} is 0.72 Å and for Ca^{2+} is 1.00 Å), whereas aragonite preferentially incorporates divalent metals with larger ionic radii, such as Sr^{2+} and Ba^{2+} (Deleuze and Brantley, 1997; Finch et al., 2001). Another common explanation is the preferential adsorption of Mg^{2+} ions onto the calcite crystal surface (Compton and Brown, 1994). Mg^{2+} ions compete with Ca^{2+} and CO_3^{2-} ions for adsorption, poisoning active growth sites such as kinks and steps (Paquette and Reeder, 1995; Fernandez-Diaz et al., 1996; Zhang and Dawe, 2000). Because Mg^{2+} has a much stronger hydration energy than Ca^{2+} (20% greater than that for Ca^{2+}), it cannot as readily be incorporated into the calcite structure and, thus, inhibits calcite growth.

Calcite was the only mineral precipitated from the 18-cycle experiment at 25^{o}C (Figure 2.6). Although inorganic calcite precipitated from natural seawater contains variable amount of $MgCO_3$, typically 8 to 18 mole % with a median of 12 mole % (Mucci and Morse, 1983; Mucci, 1987; Morse and Mackenzie, 1990; Andersson et al., 2008), given the small amount of material recovered, it was impossible to determine its magnesium content.

Results of the one-cycle experiments are consistent with those of previous studies (Sabbides and Koutsoukos, 1993; Morse et al., 1997; Pokrovsky, 1998; Waly et al., 2012), in which aragonite was shown to be the dominant mineral phase precipitating from homogeneous supersaturated seawater or solutions of high $[Mg^{2+}]$:$[Ca^{2+}]$ ratio (see Figure 2.11; Morse et al., 2007), in accordance to the Ostwald Step Rule. The literature on this topic has been reviewed by Morse et al. (2007), who also investigated factors controlling the mineralogy of the calcium carbonate that nucleates and grows from seawater under differing solution composition and temperature conditions. Calcite forms over a wide temperature range (0-35^{o}C) in Mg-free seawater, but only below about 8^{o}C in seawater of normal $[Mg^{2+}]$:$[Ca^{2+}]$ ratio (~5.2:1) (Figure 2.11).

The precipitation of calcite in our 18-cycle experiment at 25°C indicates that through multiple cycling of a solution between undersaturation and supersaturation with respect to metastable phases (aragonite), the preservation and accumulation of more stable nuclei (i.e. calcite) in solution can be achieved. Hence, according to our observations and interpretations, the mineralogy of the calcium carbonate precipitated from a supersaturated seawater solution in dynamic experiments may be controlled by differences in the kinetics of nucleation of the calcium carbonate polymorphs rather than equilibrium thermodynamics.

2.5.2 Classical and Non-Classical Calcium Carbonate Precipitation Models and Relative Induction Period of Aragonite Nucleation at 25^{o}C

Calcium carbonate provides a model system for nucleation and crystallization analysis of minerals for classical (De Yoreo and Vekilov, 2003) and non-classical (Niederberger and Cölfen, 2006; Gebauer et al., 2008) crystallization. The classical precipitation model of a solid from a supersaturated solution involves nucleation and growth. The period required for nucleation is referred to as the induction period. The induction period is affected by several factors and typically decreases with increasing saturation state, temperature, agitation speed, and the presence of impurities (organic or inorganic), seeds, or foreign particles (Söhnel and Mullin, 1978, 1982; Gomez-Morales et al., 2010; Waly et al., 2012). Several methods have been applied to determine the induction period of solid nucleation, including visual observation (Rushdi et al., 1992; Morse and He, 1993; Mullin and Osman, 1973), pH (Söhnel and Mullin, 1982; Rushdi et al., 1992; Morse and He, 1993; Pokrovsky and Savenko, 1995), turbidity (Barringer and Bowen, 1985; Soloviev et al., 2001), conductivity (Söhnel and Mullin, 1978, 1982) and calorimetry (Glasner and Tassa, 1972; Kibalczyc and Zielenkiewicz, 1987). In this study, the induction period and the onset of nucleation were established by a sharp decrease in solution pH during the, otherwise, normal increase as the CO_2-charged solution was bubbled with ambient air. A comparison of induction periods for each precipitation between 25 and 40^oC is presented in Figure 2.12, each value is the average of three replicate experiments.

No similar multi-cycle homogeneous precipitation study has ever been conducted in natural seawater, but several single-cycle studies have been (Pytkowicz, 1991; Rushdi et al., 1992, Waly et al., 2012). When comparing the induction period obtained in this study to those of similar studies (Table 2.4), it should be kept in mind that different experimental conditions could significantly affect the results. The discrepancy between induction periods observed in our study and those of Waly et al. (2012) is due to the difference in the saturation state of the experimental solutions with respect to aragonite (16 in their study compared to 3.1 in ours). At higher saturation states, the induction period is typically shorter, as documented in many studies (e.g. Söhnel and Mullin, 1978, 1982; Gomez-Morales et al., 1996; Waly et al., 2012). Rushdi et al. (1992) added 1.44 mmole/L Na_2CO_3 to artificial seawater solutions in order to increase the rate of aragonite nucleation. Although the precise saturation state of their experimental solutions was not reported, it can be calculated based on their experimental description. Given that both experiments were conducted at the same T, P and S, we estimated their solution saturation state to be 7.2 times larger ($\Omega_a \approx 22$) than in our study ($\Omega_a \approx 3.1$). Accordingly, the induction periods reported by Rushdi et al. (1992) are shorter than those of Waly et al. (2012) which, in turn, are shorter than in our study. In addition, the use of natural seawater as a parent solution during our experiments could further modify the induction period. In general, the composition of natural seawater is more complex than artificial seawater, and the presence of minor ions (e.g. Fe^{2+}, Sr^{2+}, Ba^{2+}) and dissolved organic compounds (e.g. soluble proteins, polysaccharides, humic acids) may catalyze or inhibit calcium carbonate nucleation (Treccani et al., 2006; Mucci and Morse, 1983; Waly et al., 2012; Nehrke et al., 2007; Zuddas et al., 2003).

Although the induction periods for the first few precipitation cycles in our study were nearly the same at both temperatures, they diverged at later stages of the experiments. For example, the induction period for the 18th cycle at $25^{o}C$ was approximately 11 days and it was about 7 days on the 25th cycle at $40^{o}C$. Because of the shorter induction period of nucleation at $40^{o}C$, it is reasonable to hypothesize that more stable nuclei (i.e. calcite) may not have accumulated to high enough concentrations after 25 cycles at $40^{o}C$ and more time would be required.

The classical nucleation/crystallization model is a useful concept to comprehend the nucleation phenomena, but it fails to predict observed pathways of nucleation which start with the formation pre-nucleation clusters and involve amorphous precursors (Gebauer and Cölfen, 2011; Wang et al., 2009). In the non-classical nucleation and crystallization model proposed by Gebauer et al. (2008), stable pre-nucleation ion clusters form even in undersaturated solutions. As the saturation state increases and the solution becomes supersaturated, amorphous calcium carbonate (ACC) nucleation occurs via several possible mechanisms (i.e. cluster aggregation, ion attachment, etc.). A schematic representation of the classical and non-classical view of nucleation and precipitation can be found in Figure 2.13 (Gebauer et al., 2008). To this day, no direct structural characterization of pre-nucleation clusters has been achieved, but strong indirect evidence is mounting that distinct structures are present in pre-nucleation clusters and they are related to different binding strengths in clusters. The binding strength is pH-dependent, providing for structural pre-formation of various stable clusters and nucleation to different ACC species, which later transform into specific crystalline polymorphs (Figure 2.13). In Gebauer et al. (2008), the investigated pH range was varied between pH 9 and 10. Nevertheless, despite the narrow rage investigated, an evaluation of the equilibrium ion activity products of the nucleated phases revealed that a more stable ACC (ACC I) was nucleated from stable clusters at lower pH values (pH = 9.00 to 9.50), while a less stable ACC (ACC II) was nucleated from less stable clusters at higher pH values (pH = 9.75 to 10.0). Ultimately, under ambient conditions, calcite forms from ACC I and the less stable vaterite crystallizes from ACC II (Figure 2.13, Gebauer et al., 2008).

The pre-nucleation clusters model and non-classical pathway of nucleation are new perspectives and need to be further investigated, in terms of cluster structure, composition, formation dynamics from pre-nucleation clusters to post nucleation ACC, etc. For example, the stability of clusters may also be temperature-dependent and this can be speculatively explained by entropic effects. At higher temperature, the probable release of water molecules from the hydration layer of ions caused by cluster formation may result in an increased number of degrees of freedom of the system, thus stabilizing the system (Gebauer et al., 2008). Moreover, Wang et al. (2009) reported that carboxyl-rich molecules such as acidic proteins and other biomolecules (e.g., aspartic acid, glutamic acid) could also alter the composition of pre-nucleation clusters by dehydrating Mg^{2+}, thus promoting the formation of Mg-enriched ACC that is compositionally equivalent to high-magnesium calcite and dolomite. These new insights may provide a plausible explanation that biogenic Mg-rich carbonates in sedimentary environments may be formed by non-classical processes from an amorphous precursor.

In the classical picture, nucleation is considered to take place in a solution of ions that has become supersaturated, leading to the nucleation of the solid phase by stochastic solute clustering, and the earliest crystal precursor is considered to be a cluster of critical size. In the non-classical model, stable pre-nucleation clusters form in an undersaturated solution and their conformation and stability is affected by the solution composition (and perhaps temperature). They nucleate into ACC of variable stabilities in supersaturated solutions. In turn, it is reasonable to speculate that the mineralogy of the calcium carbonate polymorph that ultimately crystallizes from a supersaturated solution will be directly affected by the structure of the pre-nucleation clusters.

2.5.3 Kinetics Factors Controlling Dolomite Precipitation

Most modern carbonates formed in normal marine environments contain no or only insignificant amounts of dolomite, although seawater is about 20 times supersaturated with respect to this mineral (Bathurst, 1975). Furthermore, it has proven difficult to experimentally precipitate dolomite below 100°C without bacterial mediation (e.g. Land, 1985; Kenward et al., 2009). The main kinetic factors which have been identified to inhibit the precipitation of dolomite below 100°C are summarized below.

(1) The high hydration energy of the magnesium ion (20% greater for Mg^{2+} than for Ca^{2+}) reduces the probability of Mg^{2+} ions incorporation in the solid and dolomite formation. Accordingly, the precipitation of Ca-rich mineral phases is favoured (Higgins and Hu, 2005; Oomori and Kitano, 1987; de Leeuw and Parker, 2001).

(2) The low activity of CO_3^{2-} in most natural solutions limits the precipitation of Mg-rich carbonates because very few carbonate ions have enough kinetic energy to penetrate the hydration barrier of Mg^{2+} (Lippmann, 1973; Warthmann et al., 2000).

(3) Certain naturally-occurring organic compounds (e.g. aspartic acid, soluble proteins) have been found to inhibit dolomite precipitation (Gaines, 1980). The inhibitory mechanism is unknown, but may include surface adsorption onto dolomite and/or complexation of the Mg^{2+} ion. Nevertheless, other organic compounds such as uric acid (produced by fermentative bacteria and an enzymatic degradation product of protein), polysaccharide, or ions like Li^+ and Fe^{2+} are believed to catalyze dolomite formation (e.g. Gullikson et al., 1961; Mansfield, 1980; Morrow, 1982; Slaughter and Hill, 1991; Zhang et al., 2012).

(4) Dissolved SO_4^{2-} has been shown experimentally to inhibit dolomite formation (Slaughter and Hill, 1991; Wright and Wacey, 2004). Nevertheless, the

role of SO_4^{2-} on dolomite formation is widely debated (e.g. Sachez-Roman et al., 2009). On the other hand, it has been proposed that both dissolved and solid sulfides, products of bacterial sulfate reduction, can catalyze Mg incorporation into the calcite lattice by decreasing the hydration/solvation energy of magnesium ions, thus promoting the nucleation and crystallization of the high-magnesian calcite and dolomite (Zhang et al., 2008; Teng et al., 2012).

The factors enumerated above may interact or counteract each other and, consequently, elucidation of the mechanism of dolomite precipitation at low temperature remains elusive. Given the numerous factors hindering the precipitation of dolomite from natural seawater below 100°C, it is not surprising that dolomite was not obtained in this study. The key to the dolomite problem is kinetics, as the presence of chemical or bacterial catalysts to dolomite formation may be critical, but this should not forestall further research on its precipitation mechanism.

2.6 Summary

In this study, water chemistry, including pH, alkalinity, and saturation state with respect to $CaCO_3$ minerals, were allowed to fluctuate to simulate the dynamic character of natural environments in order to promote dolomite formation. The Ostwald Step Rule states that a metastable solid phase will precipitate before the more stable phase, if the solution is supersaturated with respect to both the metastable and stable phases. By alternating between periods of aragonite supersaturation and undersaturation at 25°C, aragonite was obtained during the first few nucleation/precipitation cycles, but only calcite was detected in the 18th cycle of the experiments. We believe that through multiple cycles, calcite nuclei were formed and preserved at the expense of the aragonite nuclei providing enough seeds for growth during periods of supersaturation.

Similar experiments conducted at 40°C always yielded aragonite. At higher temperatures, the dehydration of Mg^{2+} should be accelerated and favour the precipitation of dolomite or magnesium calcite, yet, it has been shown that aragonite is more likely to form than calcite at higher temperature (Morse and He, 1993). Nevertheless, by alternating between periods of aragonite supersaturation and undersaturation, the metastable aragonite should have dissolved, preserving the more stable nuclei (i.e. calcite and dolomite) in solution.

In conclusion, parts of the objectives in this study—breaking the Ostwald Step Rule and synthesizing calcite from natural seawater at 25°C—were achieved, but the 40°C experiment did not yield the expected results. One of the possible explanations is that stable calcite nuclei may not have accumulated to a high enough concentration after 25 cycles at 40°C that enough calcite surfaces were available to offset the nucleation of aragonite. Another explanation may be related to the formation of stable pre-nucleation clusters, whose structure and stability depends on both solution composition and temperature, that control the nature of the nucleated ACC phase, and ultimately determine the mineralogy of the precipitated calcium carbonate polymorph.

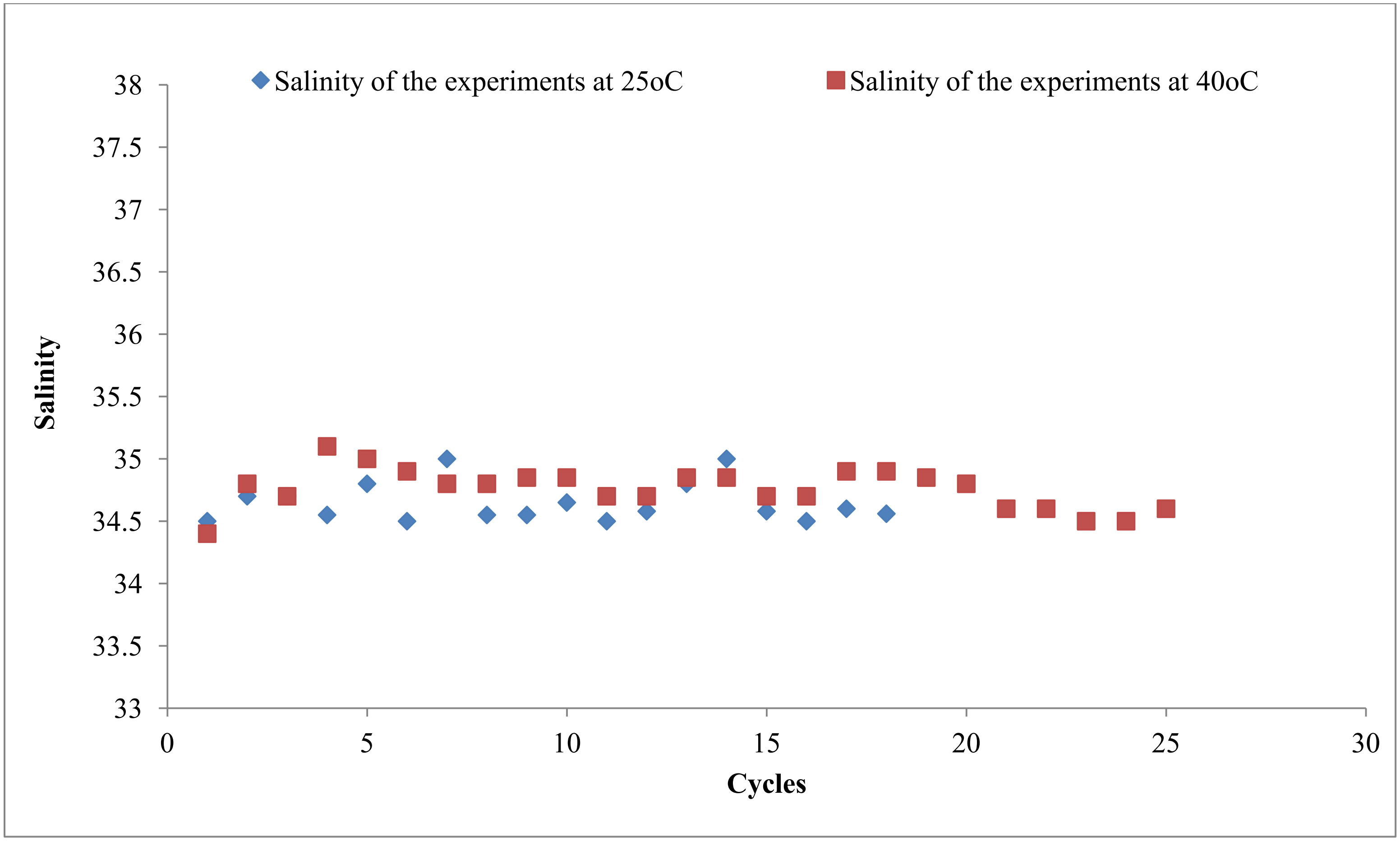

Figure 2.1 **The salinity of the seawater solutions throughout the multi-cycle experiments at 25 and 40°C.**

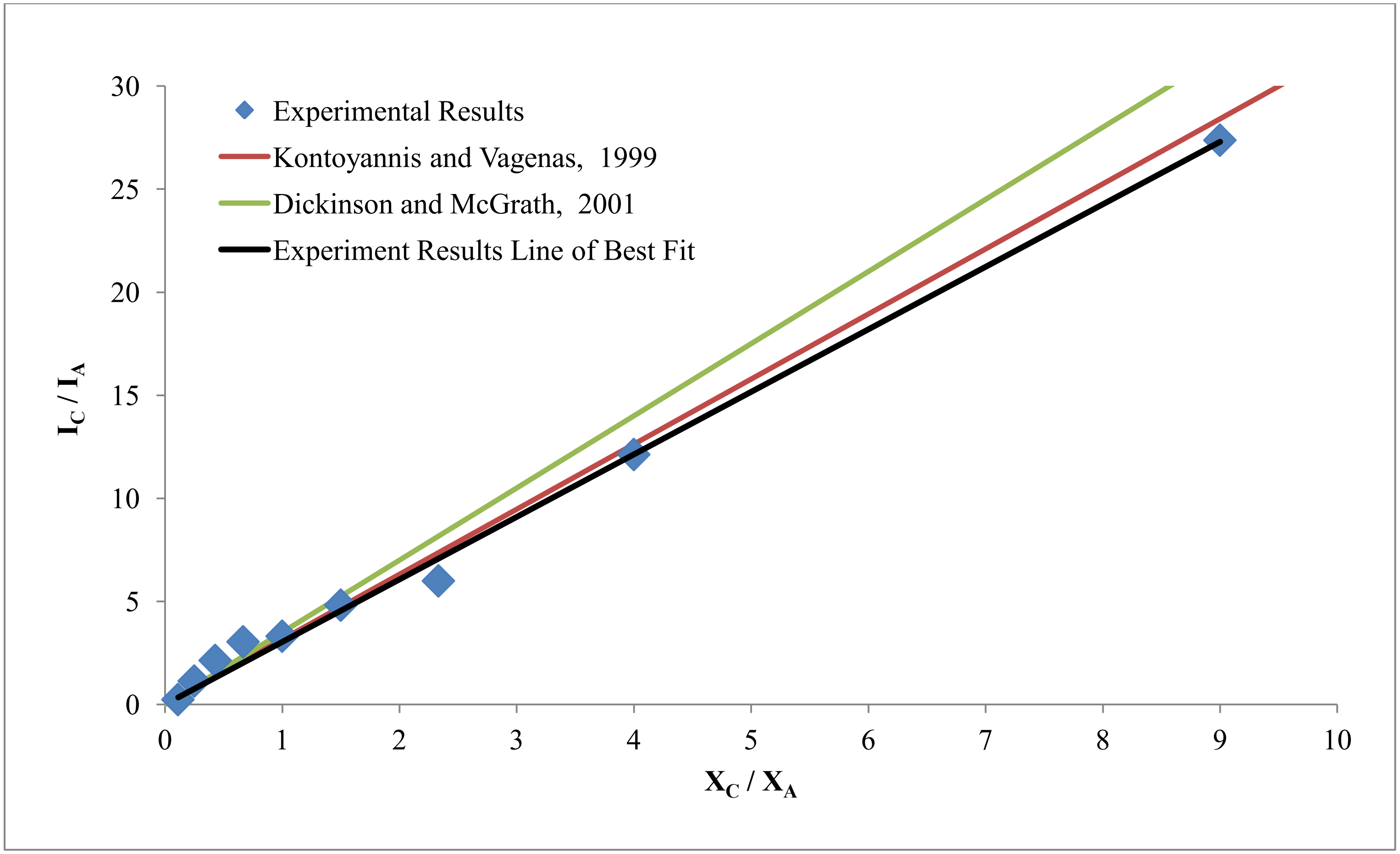

Figure 2.2 **Constructed XRD calibration curve for calcite-aragonite mixtures ($I_C/I_A = 3.034 * X_C/X_A$, $r^2 = 0.9944$) and the results of Kontoyannis and Vagenas (1999) and Dickinson and McGrath (2001).**

Table 2.1 Averaged raw data of solutions I, II, and III at 25°C. Cycles with integer numbers (i.e., 1, 2, 3, ...) represent experiments during 5 or 10% CO_2 bubbling, whereas cycles with fractional numbers (i.e., 1.5, 2.5, 3.5, ...) represent experiments during ambient-air bubbling.

Cycle	pH_{TRIS}	$[Ca^{2+}]_{diss}$ (mmol/kg)	$[Mg^{2+}]_{diss}$ (mmol/kg)	A_t (μM)	$[CO_3^{2-}]_{diss}$ (μmole/kg)	Ω_a	Ω_c	Ω_d
1	6.73	11.2	51.6	1118	64	1.0	1.6	14
1.5	8.01	9.3	52.7	2082	181	3.1	4.4	98
2	6.49	11.2	51.5	12810	43	0.7	1.0	6.2
2.5	7.98	8.9	52.8	1898	153	2.6	3.7	65
3	6.49	11.2	53.1	12610	41	0.7	1.0	6.0
3.5	7.98	8.9	52.5	1977	164	3.4	4.0	78
4	6.50	11.2	52.2	13010	44	0.7	1.1	6.7
4.5	7.96	9.0	53.2	1875	149	2.8	3.6	64
5	6.51	11.1	51.8	13310	46	0.7	1.1	7.2
5.5	7.97	9.0	53.6	1891	151	2.8	3.7	65
6	6.52	11.4	51.3	13620	48	0.8	1.2	8.0
6.5	7.97	9.0	52.3	1851	148	2.8	3.6	61
7	6.51	11.3	52.3	13410	47	0.7	1.1	7.6
7.5	7.95	8.9	52.5	1778	136	2.3	3.3	51
8	6.50	11.1	52.0	13000	44	0.7	1.1	6.5
8.5	7.97	9.0	52.3	1886	150	3.0	3.6	63
9	6.50	11.1	50.9	12900	43	0.7	1.0	6.4
9.5	7.96	9.0	52.9	1817	142	2.6	3.4	57
10	6.49	11.3	49.9	12610	41	0.7	1.0	5.7
10.5	7.98	9.1	52.1	1925	156	2.9	3.8	68
11	6.50	11.2	51.1	12900	43	0.7	1.1	6.3
11.5	7.95	8.9	51.6	1796	139	2.5	3.4	52
12	6.51	10.9	51.8	13310	46	0.7	1.1	7.0
12.5	7.94	8.9	52.6	1717	130	2.6	3.1	46

Cycle	**pH_{TRIS}**	**$[Ca^{2+}]_{diss}$ (mmol/kg)**	**$[Mg^{2+}]_{diss}$ (mmol/kg)**	**A_t (µM)**	**$[CO_3^{2-}]_{diss}$ (µmole/kg)**	**Ω_a**	**Ω_c**	**Ω_d**
13	6.51	11.2	52.4	13210	45	0.7	1.1	7.0
13.5	7.97	8.9	53.6	1802	143	2.7	3.5	58
14	6.50	11.2	52.1	13010	44	0.7	1.1	6.7
14.5	7.96	9.1	53.1	1846	145	2.7	3.5	60
15	6.52	11.4	51.7	13720	49	0.8	1.2	8.3
15.5	7.97	9.2	53.4	1880	152	2.9	3.7	67
16	6.50	11.4	52.1	13010	44	0.7	1.1	6.8
16.5	7.97	8.9	51.1	1886	151	2.9	3.7	61
17	6.51	11.3	51.6	13310	46	0.7	1.1	7.2
17.5	7.95	9.0	53.3	1802	139	2.6	3.4	55
18	6.50	11.2	51.6	13100	45	0.7	1.1	6.8
18.5	7.97	8.9	52.6	1855	147	2.8	3.5	60

Note:

pH --- measured pH on the TRIS or seawater scale;

A_t (µM) --- measured total alkalinity;

$[Ca^{2+}]_{diss}$ (mmole/kg seawater) --- measured dissolved calcium concentration;

$[Mg^{2+}]_{diss}$ (mmole/kg seawater) --- measured dissolved magnesium concentration;

$[CO_3^{2-}]_{diss}$ (µmole/kg seawater) --- calculated dissolved carbonate concentration using CO2SYS;

Ω_a --- saturation state with respect to aragonite;

Ω_c --- saturation state with respect to calcite;

Ω_d --- saturation state with respect to dolomite

Table 2.2 **Averaged raw data of solutions IV, V, and VI at 40°C. Cycles with integer numbers (i.e., 1, 2, 3, ...) represent experiments during 5 or 10% CO_2 bubbling, whereas cycles with fractional numbers (i.e., 1.5, 2.5, 3.5, ...) represent experiments during ambient-air bubbling.**

Cycle	pH_{TRIS}	$[Ca^{2+}]_{diss}$ (mmol/kg)	$[Mg^{2+}]_{diss}$ (mmol/kg)	A_t (µM)	$[CO_3^{2-}]_{diss}$ (µmole/kg)	Ω_a	Ω_c	Ω_d
1	6.62	13.0	50.3	8245	63	1.1	1.6	35
1.5	7.94	10.9	51.1	1757	209	3.7	5.3	330
2	6.40	13.1	51.0	9703	44	0.8	1.1	17
2.5	7.95	11.1	50.9	1748	212	3.7	5.3	340
3	6.38	12.9	50.4	9334	41	0.7	1.0	14
3.5	7.96	10.9	51.1	1822	226	4.0	5.7	380
4	6.39	12.9	50.6	9484	42	0.7	1.1	15
4.5	7.94	11.5	50.3	1765	210	3.7	5.3	350
5	6.41	12.7	51.3	9933	46	0.8	1.2	18
5.5	7.96	11.0	51.5	1784	220	3.8	5.5	370
6	6.38	12.5	51.1	9261	40	0.7	1.0	14
6.5	7.96	10.7	51.5	1803	223	3.9	5.6	370
7	6.38	12.8	50.8	9276	40	0.7	1.0	14
7.5	7.96	11.2	51.3	1835	230	4.0	5.8	410
8	6.39	12.2	51.0	9483	42	0.7	1.1	15
8.5	7.94	11.0	50.8	1731	205	3.6	5.2	310
9	6.38	13.0	50.6	9263	40	0.7	1.0	14
9.5	7.92	11.2	51.4	1636	187	3.3	4.7	270
10	6.36	12.6	51.7	8910	37	0.7	0.9	12
10.5	7.94	11.0	51.4	1697	201	3.5	5.1	310
11	6.37	12.6	51.3	9126	39	0.7	1.0	13
11.5	7.94	10.8	51.4	1736	207	3.6	5.2	320
12	6.38	12.9	51.2	9334	41	0.7	1.0	15

Cycle	**pH_{TRIS}**	**$[Ca^{2+}]_{diss}$ (mmol/kg)**	**$[Mg^{2+}]_{diss}$ (mmol/kg)**	**A_t (μM)**	**$[CO_3^{2-}]_{diss}$ (μmole/kg)**	**Ω_a**	**Ω_c**	**Ω_d**
12.5	7.95	10.9	51.5	1759	212	3.7	5.3	340
13	6.38	11.6	50.4	9272	40	0.7	1.0	13
13.5	7.95	10.9	50.9	1779	215	3.8	5.4	350
14	6.38	12.1	50.3	9409	41	0.7	1.0	14
14.5	7.95	10.9	51.2	1757	214	3.7	5.4	340
15	6.36	12.7	51.4	8981	38	0.7	1.0	12
15.5	7.93	11.2	51.5	1694	198	3.5	5.0	300
16	6.38	12.9	51.0	9335	41	0.7	1.0	15
16.5	7.94	11.7	51.0	1765	212	3.7	5.3	360
17	6.39	13.0	51.0	9560	43	0.7	1.1	16
17.5	7.94	10.9	51.0	1742	209	3.7	5.3	330
18	6.38	12.9	50.9	9262	40	0.7	1.0	14
18.5	7.87	11.1	51.1	1445	159	2.8	4.0	220
19	6.40	12.6	51.0	9780	44	0.8	1.1	17
19.5	7.93	11.3	51.1	1694	199	3.5	5.0	310
20	6.39	12.5	50.6	9628	43	0.8	1.1	16
20.5	7.94	11.3	51.0	1703	202	3.5	5.1	320

Note:

pH --- measured pH on the TRIS or seawater scale;

A_t (μM) --- measured total alkalinity;

$[Ca^{2+}]_{diss}$ (mmole/kg seawater) --- measured dissolved calcium concentration;

$[Mg^{2+}]_{diss}$ (mmole/kg seawater) --- measured dissolved magnesium concentration;

$[CO_3^{2-}]_{diss}$ (μmole/kg seawater) --- calculated dissolved carbonate concentration using CO2SYS;

Ω_a --- saturation state with respect to aragonite;

Ω_c --- saturation state with respect to calcite;

Ω_d --- saturation state with respect to dolomite

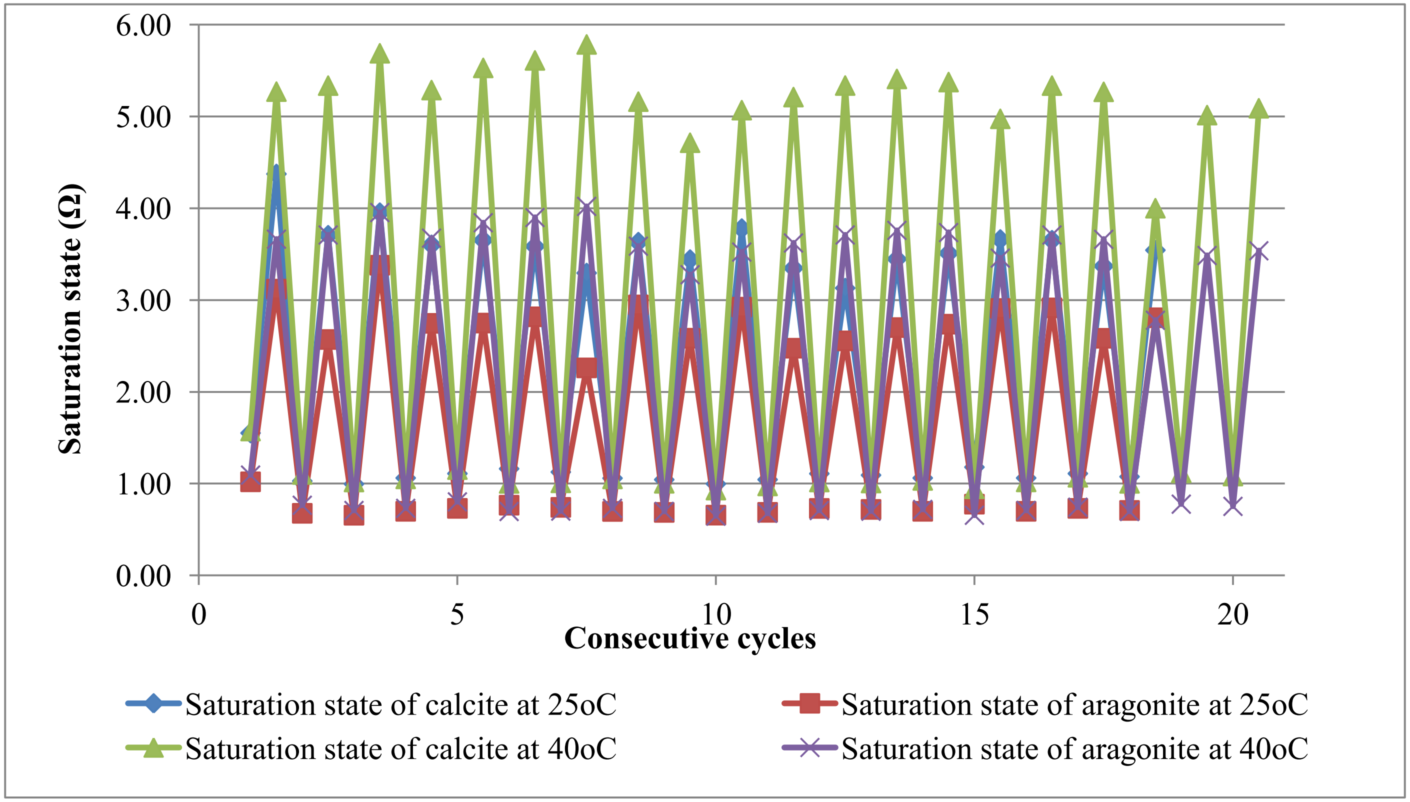

Figure 2.3 **Experimental solution saturation states with respect to calcite and aragonite throughout the consecutive bubbling cycles at 25 and 40°C. At 25°C, 18 bubbling cycles were conducted whereas 20 bubbling cycles were carried out at 40°C. The minima of each curve occurred during CO_2/N_2 bubbling, whereas the maxima of each curve occurred during ambient-air bubbling.**

Table 2.3 Total ion activity coefficients of Ca^{2+}, Mg^{2+} and CO_3^{2-} in seawater used in this study. (Millero and Pierrot, 1998)

Temperature(^oC)	Ca^{2+}	Mg^{2+}	CO_3^{2-}
25	0.198	0.203	0.043
40	0.188	0.191	0.039

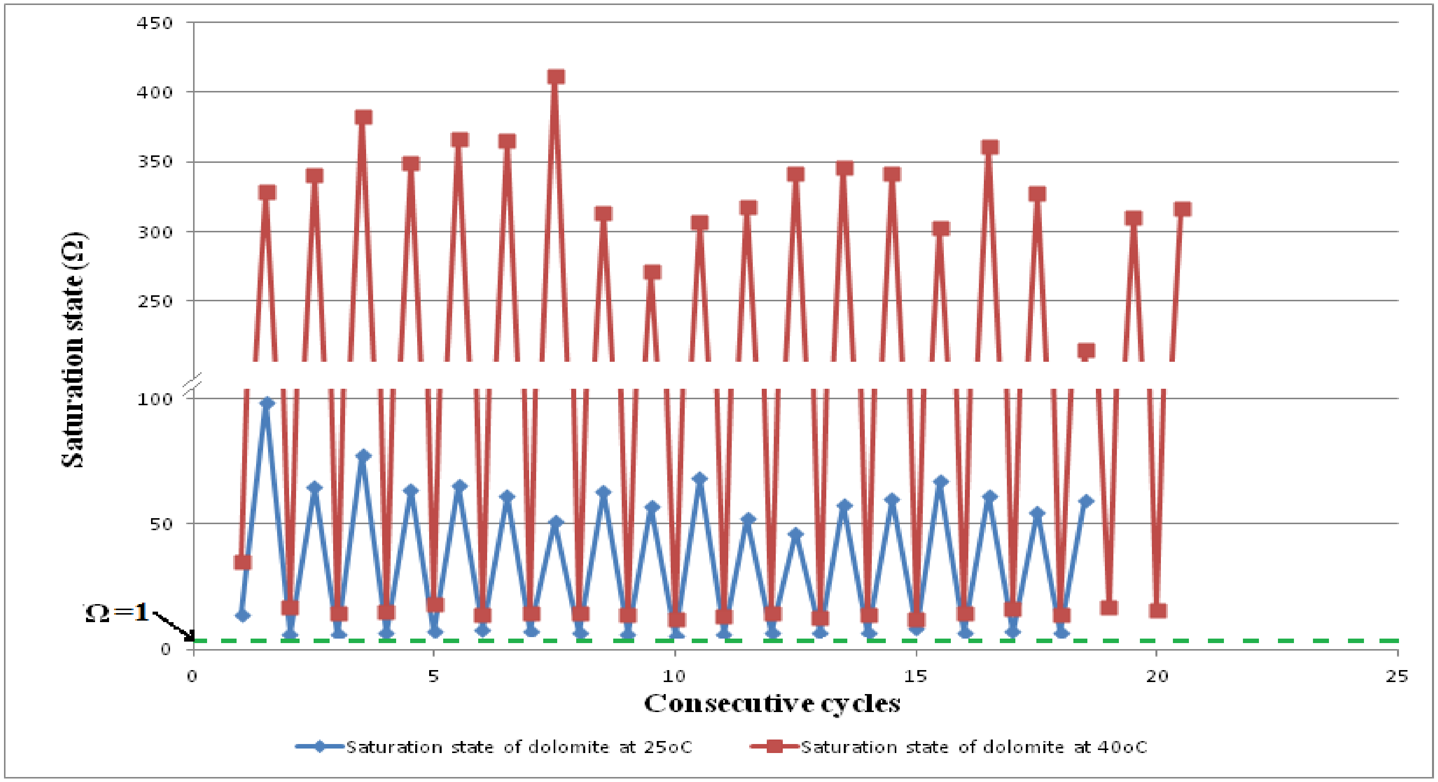

Figure 2.4 **Experimental solution saturation states with respect to dolomite throughout the consecutive bubbling cycles at 25 and 40°C. At 25°C, 18 bubbling cycles were conducted whereas 20 bubbling cycles were carried out at 40°C. The minima of each curve occurred during CO_2/N_2 bubbling, whereas the maxima of each curve occurred during ambient-air bubbling. The green dash line indicates the equilibrium with respect to dolomite (Ω_d =1). The solutions remained supersaturated (Ω_d >1) with respect to dolomite during both CO_2/N_2 and ambient-air bubbling.**

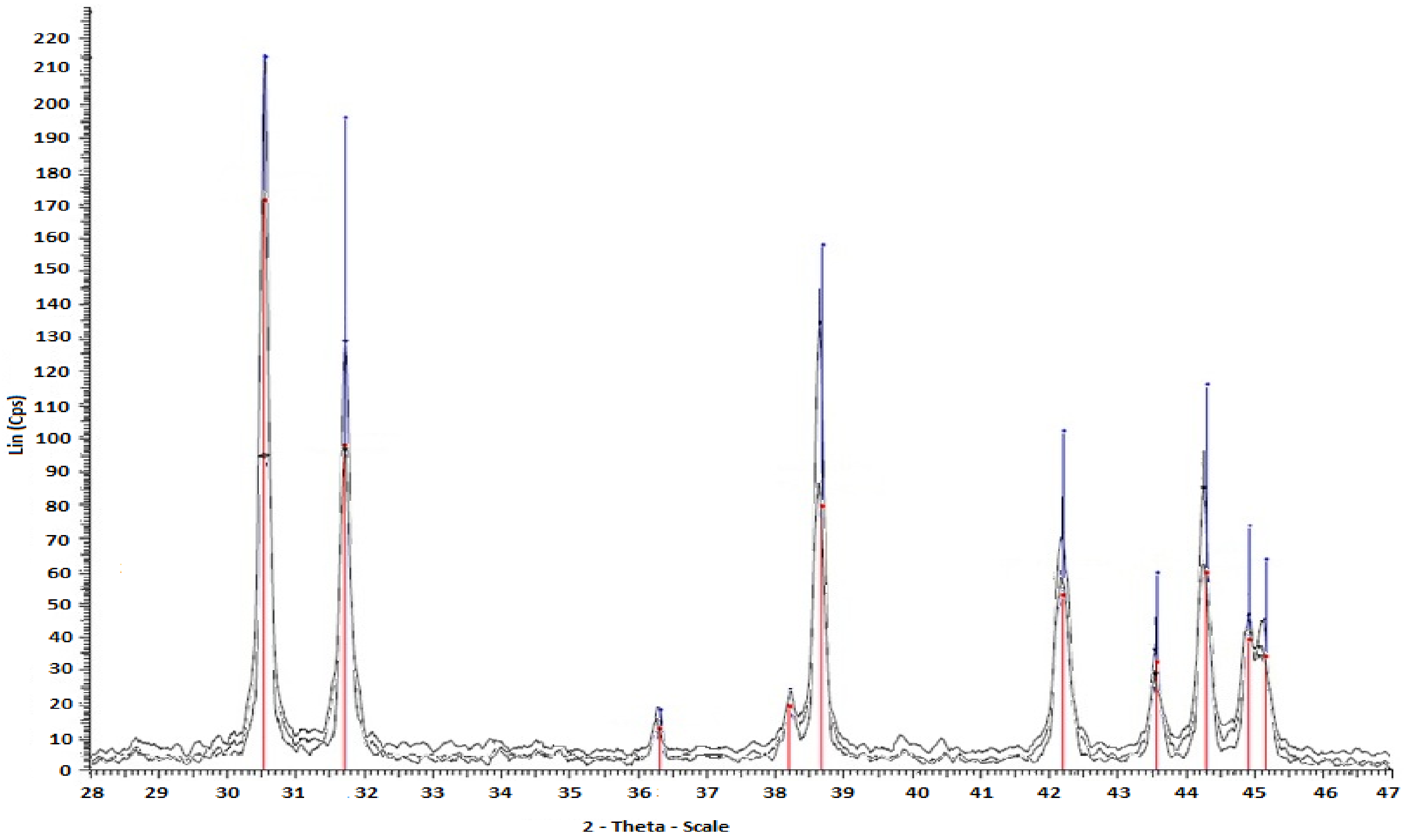

Figure 2.5 X-ray powder diffractogram of the precipitates formed after the 1st cycle at 25°C. Aragonite was the only mineral observed in the precipitate. Triplicate experiments yielded identical results.

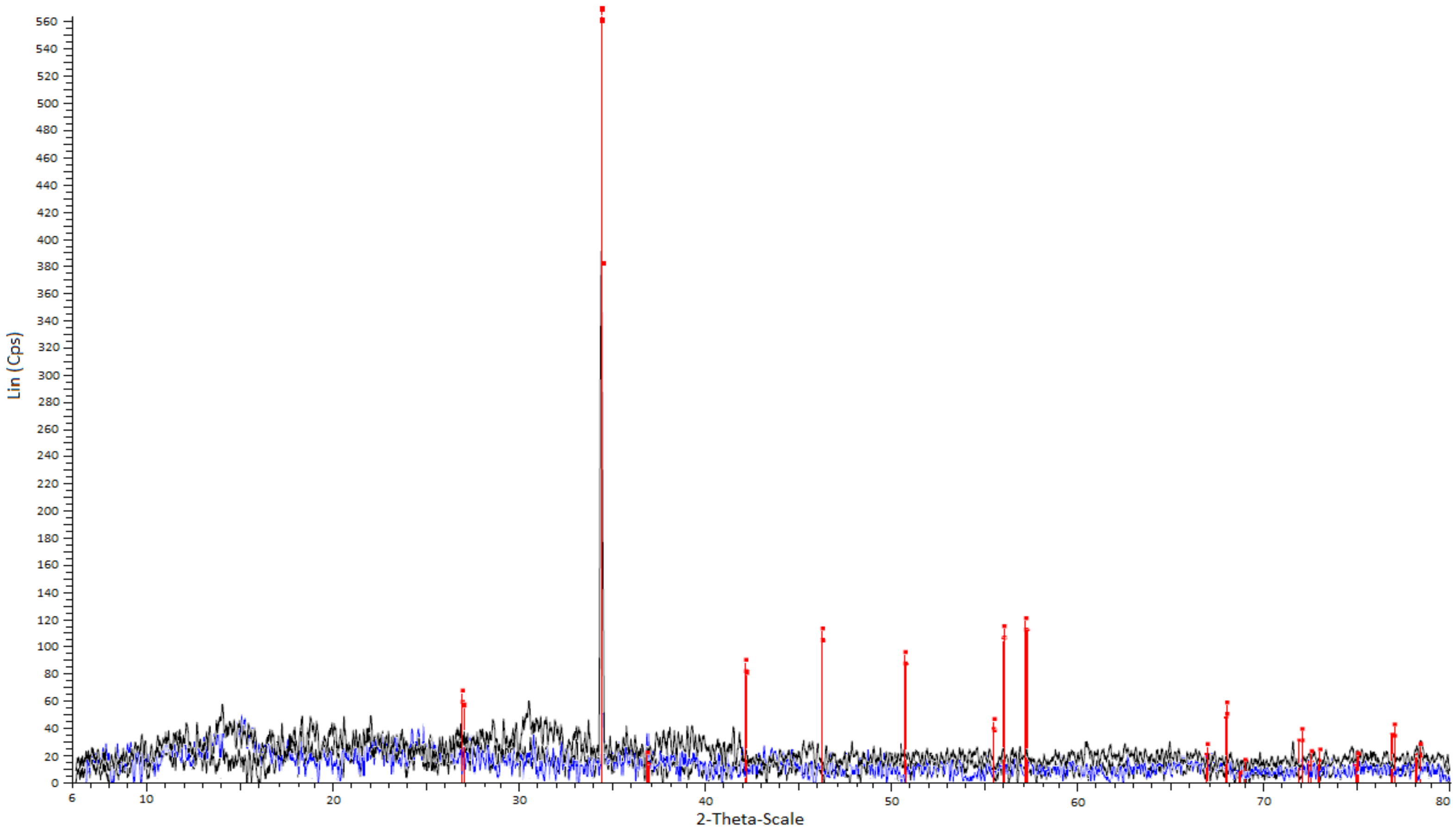

Figure 2.6 X-ray powder diffractogram of the precipitate formed after the 18th cycle at 25°C. Calcite was the only mineral observed in the precipitate. Triplicate experiments yielded identical results.

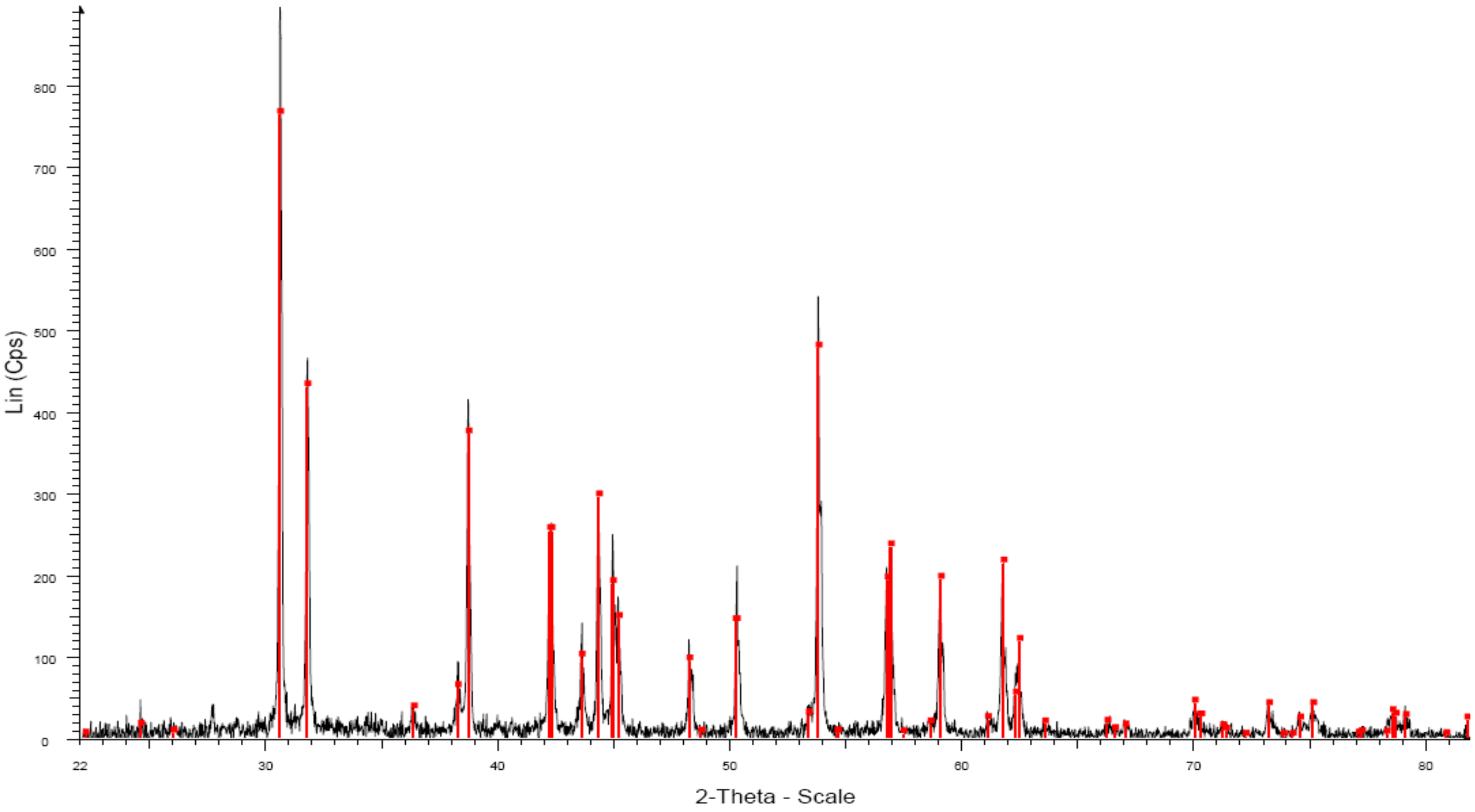

Figure 2.7 **X-ray powder diffractogram of the precipitate formed after a single 10-cycle experiment at 25°C. Aragonite was the only mineral observed in the precipitate.**

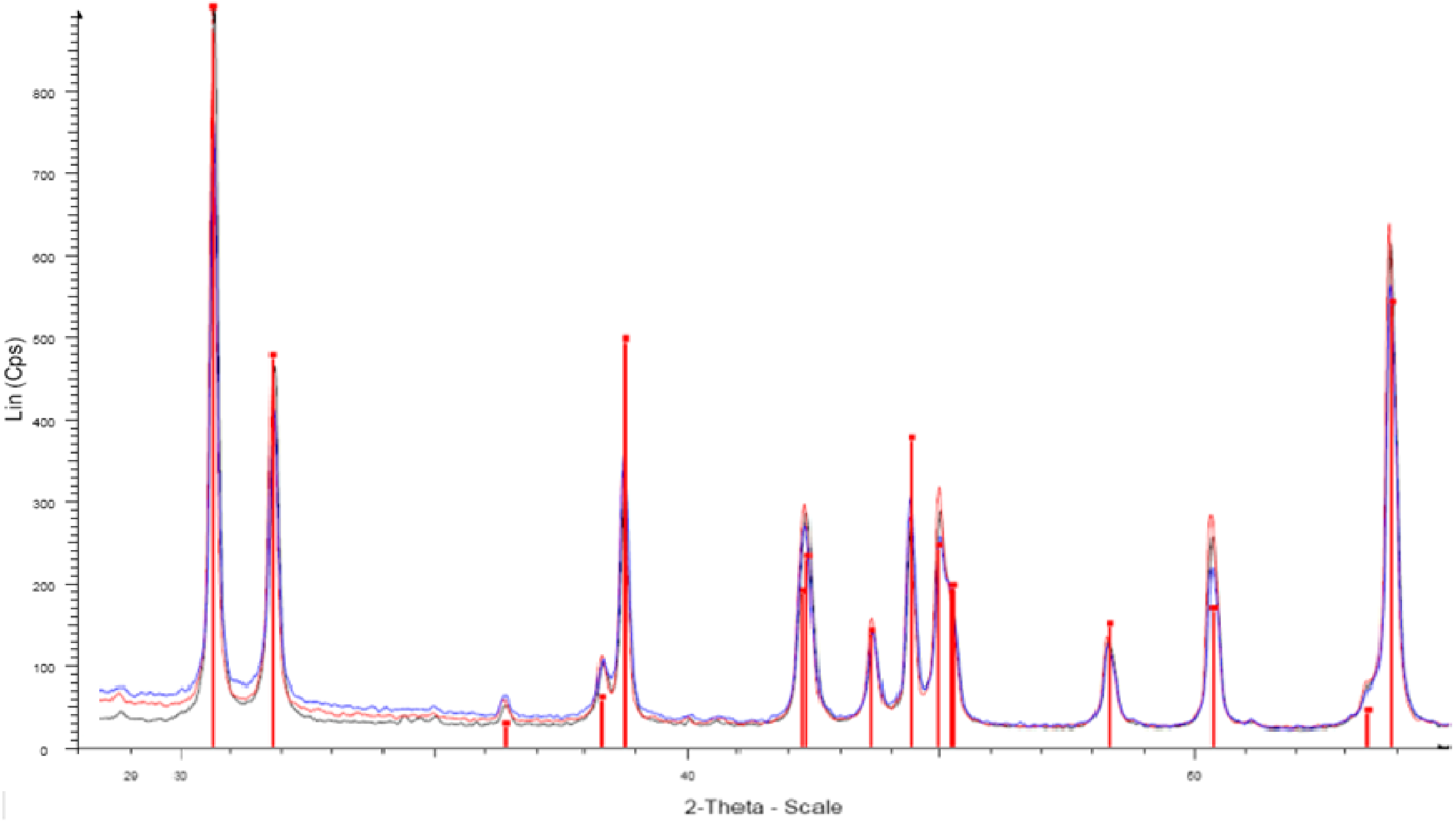

Figure 2.8 X-ray powder diffractogram of the precipitate formed after the 1st cycle at 40°C. Aragonite was the only mineral observed in the precipitate. Triplicate experiments yielded identical results.

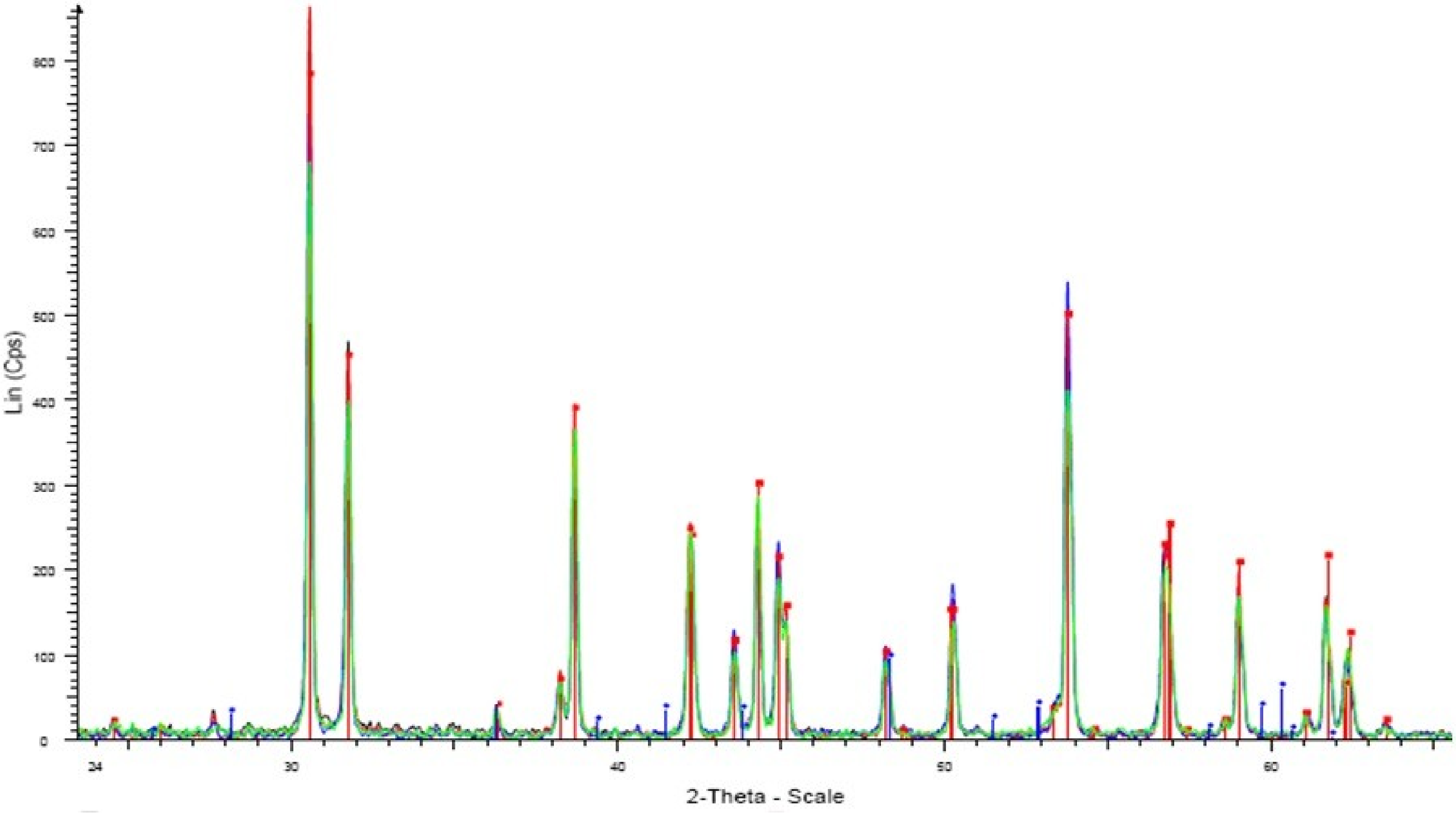

Figure 2.9 **X-ray powder diffractogram of the precipitate formed after the 20th cycle at 40°C. Aragonite was the only mineral observed in the precipitate. Triplicate experiments yielded identical results.**

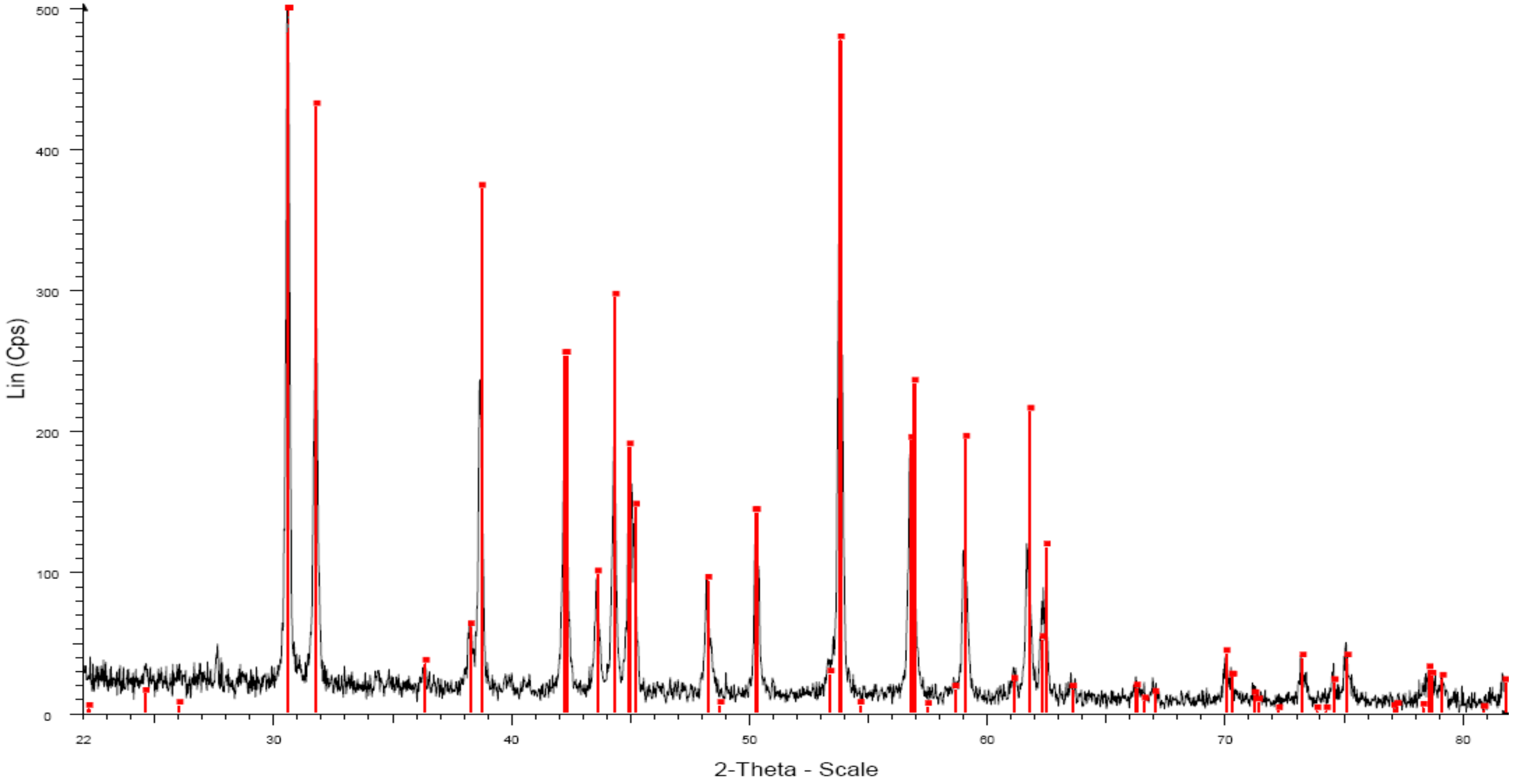

Figure 2.10 X-ray powder diffractogram of the precipitate formed after a single 25-cycle experiment at 40°C. Aragonite was the only mineral observed in the precipitate.

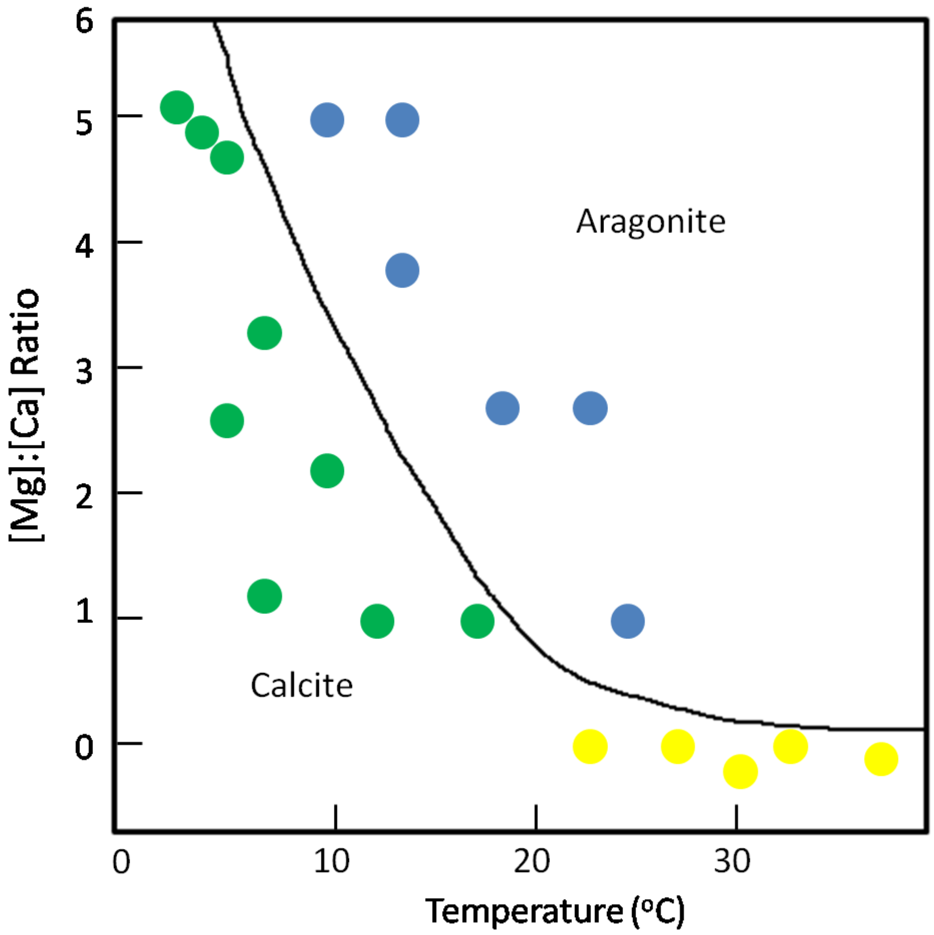

Figure 2.11 Influences of seawater $[Mg^{2+}]:[Ca^{2+}]$ ratio and temperature on the nucleation of calcium carbonate from seawater. Blue circles are aragonite; yellow circles are calcite; green circles are initially calcite with aragonite overgrowths. (reproduced from Morse et al., 2007).

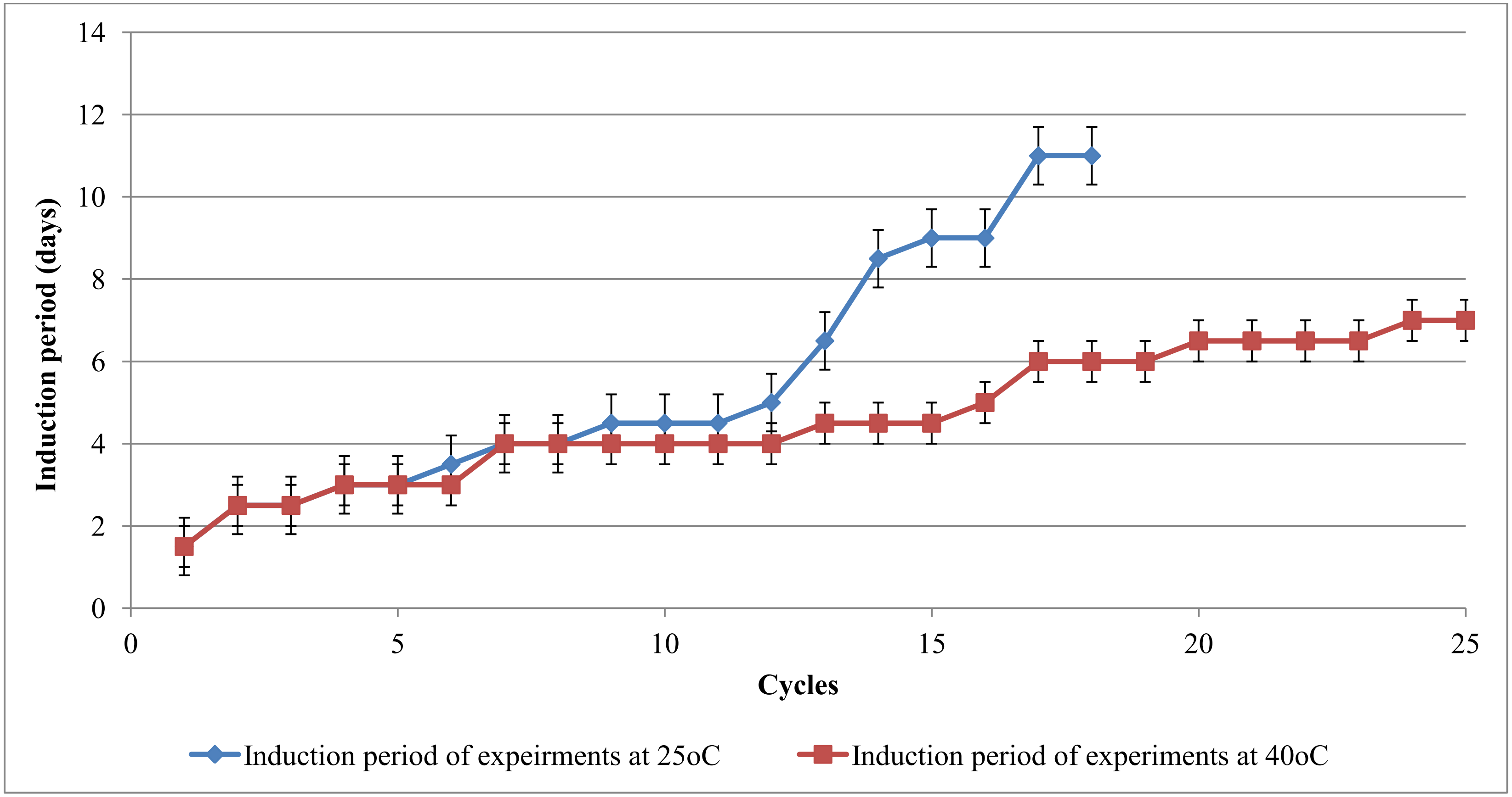

Figure 2.12 Approximate induction periods for nucleation in experiments carried out at 25 and 40°C. Although the induction periods during the first few cycles at both temperatures are approximately the same, the induction period for the last 4-5 cycles of the 18-cycle experiment at 25°C is much longer than that at 40°C.

Table 2.4 Compilation of aragonite nucleation induction periods taken from the literature and measured in this study at 25°C.

Parent Solution	Induction Period (mins)	Saturation State	Mineralogy	Temperature (°C)	Reference
Artificial seawater with $[Mg^{2+}]:[Ca^{2+}]=5$, with addition of 1.44 mmole/L Na_2CO_3	360	$\Omega_a=22$	Aragonite	25	Rushdi et al., 1992
Natural seawater with 8.25 mmole/L Na_2CO_3	1020	Unknown	Calcium Carbonate (Mineralogy was not specified)	24	Pytkowicz, 1991
30% recovery for the desalination plant in the Gulf of Oman ($[Mg^{2+}]:[Ca^{2+}]=4.7$)	600	$\Omega_a=16$	Aragonite	20	Waly et al., 2012
50% recovery for the desalination plant in the Gulf of Oman ($[Mg^{2+}]:[Ca^{2+}]=4.7$)	900	$\Omega_a=16$	Aragonite	20	Waly et al., 2012
Natural seawater($[Mg^{2+}]:[Ca^{2+}]=5.2$)	2160	$\Omega_a=3.1$	Aragonite	25	This study

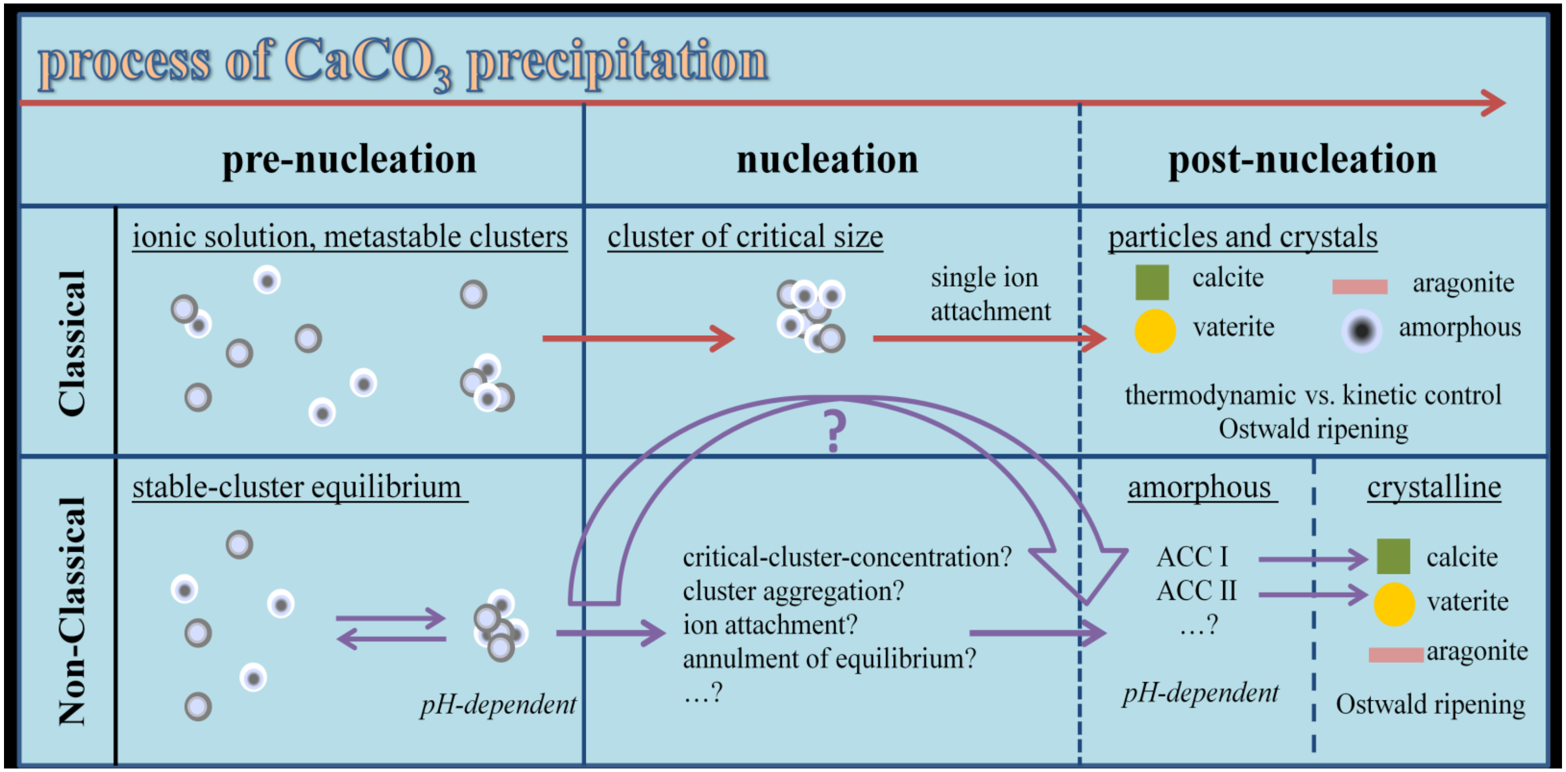

Figure 2.13 Schematic representations of the classical and non-classical view of precipitation (not to scale). Pre-nucleation stage calcium carbonate clusters provide an early precursor species of different ACC phases giving rise to an alternative crystallization-reaction channel. (reproduced from Gebauer et al., 2008).

2.7 References

Akin, G.W. and Lagerwerff, J.V. (1965) Calcium carbonate equilibria in aqueous solutions open to the air. Ll. Enhanced solubility of $CaCO_3$ in the presence of Mg^{2+} and SO_4^{2-}. *Geochim. Cosmochim. Acta* **29**, 353–360

Andersson, A.J., Mackenzie, F.T. and Bates, N.R. (2008) Life on the margin: implications of ocean acidification on Mg-calcite, high latitude and cold-water marine calcifiers. *Mar. Ecol. Prog. Ser.* **373**, 265-273

Arrhenius, S.Z. (1889) *phys. Chem*. **4**, 226; a translation of the four pages in this paper that deal with temperature dependence is included in Back, M.H., and Laidler, K.J., "Selected Readings in Chemical Kinetics," Pergamon Press, Oxford, 1967, pp. 31-35.

Arvidson, R.S. and Mackenzie, F.T. (1999) The dolomite problem: control of precipitation kinetics by temperature and saturation state. *Am. J. Sci*. **299**, 257-288

Barringer, E.A. and Bowen, H.K. (1985) High-purity, monodisperse TiO_2 powders by hydrolysis of titanium tetraethoxide. 1. Synthesis and physical properties. *Langmuir* **1**, 414-420

Bathurst, R.G.C. (1975) Carbonate sediments and their diagenesis. Developments in Sedimentology. Elsevier, Amsterdam, pp. 658.

Berner, R.A. (1975) The role of magnesium in the crystal growth of calcite and aragonite from sea water. *Geochim. Cosmochim. Acta* **39,** 489–504

Chai, L., Navrotsky, A. and Reeder, R.J. (1995) Energetics of calcium-rich dolomite. *Geochim. Cosmochim. Acta* **5**, 939-944

Chilingar, G.V. (1956) Relationship between Ca/Mg ratio and geological age. *Bull. Am. Ass. Petrol. Geol.* **40**, 2256-2266

Choudens-Sánchez, V.D. and González, L.A. (2009) Calcite and aragonite precipitation under controlled instantaneous supersaturation: Elucidating the role of $CaCO_3$ saturation state and Mg/Ca ratio on calcium carbonate polymorphism. *J. Sediment. Res*. **79**, 363-376

Compton, R.G. and Brown, C.A. (1994) The inhibition of calcite dissolution/precipitation: Mg^{2+} cations. *J. Colloid Interface Sci.* **165**, 445–449

Davis, K.J., Dove, P.M., Wasylenki L.E. and Yoreo J.J. (2004) Morphological consequences of differential Mg^{2+} incorporation at structurally distinct steps on calcite. *Am. Mineral.* **89**, 714-720 de Leeuw, N.H. and Parker, S.C. (2001) Surface-water interactions in the dolomite problem. *Phys. Chem. Chem. Phys.* **3**, 3217–3221

Deelman, J.C. (1999) Low-temperature nucleation of magnesite and dolomite. *N. Jb. Miner. Mh*. **7**, 289-302

Deelman, J.C. (2001) Breaking Ostwald's rule. *Chem. Erde* **61**, 224-235

Deleuze, M. and Brantley, S. L. (1997) Inhibition of calcite crystal growth by Mg^{2+} at 100°C and 100 bars: Influence of growth regime. *Geochim. Cosmochim. Acta* **61**, 1475–1485

De Yoreo, J.J. and Vekilov, P.G. (2003) Principles of crystal nucleation and growth. *Rev Mineral Geochem* **54**, 57-93

Dickinson, S.R. and McGrath, K.M. (2001) Quantitative determination of binary and tertiary calcium carbonate mixtures using powder X-ray diffraction. *Analyst* **126**, 1118-1121

dos Anjos, A.P.A., Sifeddine, A., Sanders, C.J. and Patchineelam, S.R. (2011) Synthesis of magnesite at low temperature. *Carbonates and Evaporites* **26**, 213-215

Fernandez-Diaz, L., Putnis, A., Prieoto, M. and Putnis, C.V. (1996) The role of magnesium in the crystallization of calcite and aragonite in a porous medium. *J. Sediment. Res.* **66**, 482–491

Finch, A.A., Shaw, P.A., Weedon, G.P. and Holmgren, K. (2001) Trace element variation in speleothem aragonite: potential for palaeoenvironmental reconstruction. *Earth Planet. Sci. Lett.* **186**, 255-267

Gaines, A.M. (1980) Dolomitization kinetics, recent experimental studies. In: Concepts and Models of Dolomitization (Eds. D.H. Zenger, J.B. Dunham and R.L. Ethington) *Soc. Econ. Paleontol. Mineral. Spec. Publ*. **28**, 81-86

Garrels, R.M., Thompson, M.E. and Siever, R. (1960) Stability of some carbonates at 25^{o}C and one atmosphere total pressure. *Am. J. Sci.* **258**, 402-418

Gebauer, D. and Cölfen, H. (2011) Prenucleation clusters and non-classical nucleation. *Nano Today* **6**, 564-584

Gebauer, D., Völkel, A. and Cölfen, H. (2008) Stable prenucleation calcium carbonate clusters. *Science* **322**, 1819-1822

Glasner, A. and Tassa, M. (1972) The thermal effects of nucleation and crystallization of KBr solutions. *J. Cryst. Growth* **13/14**, 441-444

Gomez-Morales, J., Torrent-Burgues, J. and Rodriguez-Clemente, R. (1996) Nucleation of calcium carbonate at different initial pH conditions. *J. Cryst. Growth* **169**, 331-338

Gomez-Morales, J., Hernandez-Hernandez, A., Sazaki, G. and Garciz-Ruiz, J.M. (2010) Nucleation and polymorphism of calcium carbonate by a vapor diffusion sitting drop crystallization technique. *Cryst. Growth Design* **10**, 963-969

Grasshoff, K. (1964) On the determination of silica in sea water. *Deep-Sea Res.* **11**, 597-604

Gullikson, D.M., Caraway, W.H. and Gates, G.L. (1961) Chemical analysis and electrical resistivity of selected California oil field waters. *U.S. Bur. Mines Rept. Inv*. **5736**, 21.

Hemingway, B.S. and Robie, R.A. (1994) Enthalpy and Gibbs energy of formation of dolomite, $CaMg(CO_3)_2$, at 298.15 K from HCl solution calorimetry. *U.S. Geol. Surv. Open-file report* 94-575. U.S. Geological Survey, Reston, VA.

Higgins, S.R. and Hu, X.M. (2005) Self-limiting growth on dolomite: Experimental observations with in situ atomic force microscopy. *Geochim. Cosmochim. Acta* **69**, 2085-2094

James, N.P. and Clarke, J. (1997) Cool-water carbonates. *SEPM Special Publication* **56**, 440

Katz, A., Sass, E., Starinsky, A. and Holland, H.D. (1972) Strontium behavior in the aragonite-calcite transformation: an experimental study at 40-98^{o}C. *Geochim. Cosmochim. Acta* **36**, 481-496

Kawano, J., Shimobayashi, N., Miyake, A. and Kitamura, M. (2009) Precipitation diagram of calcium carbonate polymorphs: its construction and significance. *J. Phys. Condens. Matter* **21**, 1-6

Kenward, P.A., Goldstein, R.H., Gonzalez, L.A. and Roberts, J.A. (2009) Precipitation of low-temperature dolomite from an anaerobic microbial consortium: the role of methanogenic Archaea. *Geobiology* **7**, 556-565

Kibalczyc, W. and Zielenkiewicz, A. (1987) Calorimetric investigations of calcium phosphate precipitation in relation to solution composition and temperature. *Thermochim. Acta* **131**, 47-55

Kitano, Y., Park, K. and Hood, D.W. (1962) Pure aragonite synthesis. *J. Geophys. Res.* **67**, 4873–4874

Kontoyannis, C.G. and Vagenas, N.V. (2000) Calcium carbonate phase analysis using XRD and FT-Raman spectroscopy. *Analyst* **125**, 251-255

Krause, S., Liebetrau, V., Gorb, S., Sánchez-Román, M., McKenzie, J.A. and Treude, T. (2012) Microbial nucleation of Mg-rich dolomite in exopolymeric substances under anoxic modern seawater salinity: New insight into an old enigma. *Geology* **40**, 587-590

Land, L.S. (1985) The origin of massive dolomite. *J. Geol. Educ.* **33**, 112-125

Land, L.S. (1998) Failure to precipitate dolomite at 25°C from dilute solution despite 1000-fold oversaturation after 32 years. *Aquat. Geochem.* **4**, 361-368

Lin, Y. and Singer, P.C. (2009) Effect of Mg^{2+} on the kinetics of calcite crystal growth. *J. Cryst. Growth* **312**, 136-140

Lippmann, F. (1973) Sedimentary Carbonate Minerals. Springer-Verlag, Berlin, pp. 228.

Lopez, O., Zuddas, P. and Faivre, D. (2009) The influence of temperature and seawater composition on calcite crystal growth mechanisms and kinetics: Implications for Mg incorporation in calcite lattice. *Geochim. Cosmochim. Acta* **73**, 337-347

Mansfield, C.F. (1980) A urolith of biogenic dolomite - another clue in the dolomite mystery. *Geochim. Cosmochim. Acta* **44**, 829-839

McGregor, H. V. and Gagan, M. K. (2003) Diagenesis and geochemistry of Porites corals from Papua New Guinea: implications for paleoclimate reconstruction. *Geochim. Cosmochim. Acta* **67**, 2147–2156

McKenzie, J.A. (1991) The dolomite problem: An outstanding controversy. In: Controversies in Modern Geology. (Eds. D.W. Muller) Academic Press, New York, pp. 490.

Millero, F.J. (1996) Chemical Oceanography. CRC Press, Boca Raton, pp.63-67.

Millero, F.J. and Pierrot, D. (1998) A chemical equilibrium model for natural waters. *Aquat. Geochem.***4**, 153-199

Millero, F.J., Zhang, J.Z., Fiol, S., Sotolongo, S., Roy, R.N., Lee, K. and Mane, S.(1993) The use of buffers to measure the pH of seawater. *Mar. Chem.* **44**, 143–152

Morrow, D.W. (1982) Diagenesis I. Dolomite-part I: The chemistry of dolomitization and dolomite precipitation. *Geosci. Can.* **9**, 5-13

Morse, J.W., Arvidson, R.S. and Lüttge, A. (2007) Calcium carbonate formation and dissolution. *Chem. Rev.* **107**, 342–381

Morse, J.W. and He, S. (1993) Influences of T, S and PCO_2 on the pseudo-homogeneous precipitation of $CaCO_3$ from seawater: implications for whiting formation. *Mar. Chem.* **41**, 291-297

Morse, J.W. and Mackenzie, F.T. (1990) Geochemistry of Sedimentary Carbonates. Elsevier, New York, Amsterdam, pp.707.

Morse, J.W., Wang, Q. and Tsio, M.Y. (1997) Influences of temperature and Mg:Ca ratio on $CaCO_3$ precipitates from seawater. *Geology* **25**, 85-87

Mucci, A. (1983) The solubility of calcite and aragonite in seawater at various salinities, temperatures, and one atmosphere total pressure. *Am. J. Sci.* **283**, 780-799

Mucci, A. (1987) Influence of temperature on the composition of magnesian calcite overgrowths precipitated from seawater. *Geochim. Cosmochim. Acta* **51**, 1977–1984

Mucci, A. and Morse, J.W. (1983) The incorporation of Mg^{2+} and Sr^{2+} into calcite overgrowths: influences of growth rate and solution composition. *Geochim. Cosmochim. Acta* **47**, 217–233

Mullin, J.W. and Osman, M.M. (1973) The nucleation and precipitation of nickel ammonium sulphate crystals from aqueous solution. *Krist. Technik.* **8,** 471-481

Murphy, J. and Riley, J.P. (1962) A modified single solution method for the determination of phosphate in natural waters. *Anal. Chim. Acta* **27**, 31-36

Nancollas, G.H. (1982) Phase transformation during precipitation of calcium salts. In: Biological Mineralization and Demineralization (Eds. G. H. Nancollas), Springer-Verlag, pp. 79–99.

Nancollas, G.H., Sawada, K. and Schuttringer, E. (1983) Mineralization reactions involving calcium carbonates and phosphates. In: Biomineralization and Biological Metal Accumulation (Eds. P. Westbroek and E.W De Jong.), pp. 155–169.

Nehrke, G., Reichart, G.J., Van Cappellen, P., Meile, C. and Bijma, J. (2007) Dependence of calcite growth rate and Sr partitioning on solution stoichiometry: non-kossel crystal growth. *Geochim. Cosmochim. Acta* **71**, 2240-2249

Niederberger, M. and Cölfen, H. (2006) Oriented attachment and mesocrystals: Non-classical crystallization mechanisms based on nanoparticle assembly. *Phys. Chem. Chem. Phys*. **8**, 3271-3287

Oomori, T. and Kitano, Y. (1987) Synthesis of protodolomite from sea-water containing dioxane. *Geochem. J.* **21**, 59–65

Oppenheimer, C.H. and Master, M. (1965) On the solution of quartz and precipitation of dolomite in sea water during photosynthesis and respiration. *Zeitsch. Allg. Midrobiologie* **5**, 48-51

Ostwald, W.Z. (1897) Studien uber die Bildung und Umwaldung fester Korper. I. Abhandlung: Ubersattigung and Uberkaltung: Zeitschr. *Physik Chemie*. **22**, 289-330

Paquette, J. and Reeder, R.J. (1995) Relationship between surface structure, growth mechanism and trace element incorporation in calcite. *Geochim. Cosmochim. Acta* **59**, 735–749

Perdikouri, C., Kasioptas, A., Geiser, T., Schmidt, B.C. and Putnis, A. (2011) Experimental study of the aragonite to calcite transition in aqueous solution. *Geochim. Cosmochim. Acta* **75**, 6211-6224

Pokrovsky, O.S. (1998) Precipitation of calcium and magnesium carbonates from homogeneous supersaturated solutions. *J. Cryst. Growth* **186**, 233-244

Pokrovsky, O.S. and Savenko, V.S. (1995) Kinetics of calcium carbonate nucleation in seawater: the role of phosphates and hydrodynamics of the medium. *Oceanology* **35**, 599-603

Purser, B.H., Tucker, M.E. and Zenger, D.H. (1994) Problems, progress and future research concerning dolomites and dolomitization. In: Dolomites: A Volume in Honour of Dolomieu (Eds. B.H. Purser, M.E. Tucker and D.H. Zenger), Blackwell Scientific Publications, Oxford, pp. 3–28.

Pytkowicz, R.M. (1991) Activity coefficients in electrolyte solutions. CRC Press, West Palm Beach, Vols. 1 and 2.

Rao, C.P. (1990) Petrography, trace elements and oxygen and carbon isotopes of Gordon Group carbonates (Ordovician), Florentine Valley, Tasmania, Australia. *Sediment. Geol*. **66**, 83-97

Reddy, M.M. and Wang, K.K. (1980) Crystallization of calcium carbonate in the presence of metal ions. I. Inhibition by magnesium ion at pH 8.8 and 25°C. *J. Cryst. Growth* **50**, 470–480

Reeder, R.J. (1983) Crystal chemistry of the rhombohedral carbonates. *Rev. Mineral. Geochem*. **11**, 1-47

Robie, R.A., Hemingway, B.S. and Fisher, J.R. (1979) Thermodynamic Properties of Minerals and Related Substances at 298.15K and 1Bar (10^5 Pascals) Pressure and at Higher Temperatures. Geol. Survey Bull. 1452. U.S. Gov. Printing Office, Washington, D.C., pp.456.

Rodriguez-Blanco, J.D., Shaw, S. and Benning, L.G. (2011) The kinetics and mechanisms of amorphous calcium carbonate (ACC) crystallization to calcite, via vaterite. *Nanoscale* **3**, 265-271

Ronov, A.B. (1964) Common tendencies in the chemical evolution of the Earth's crust, ocean and atmosphere. *Geochem. Int*. **4**, 713-737

Rushdi, A.I., Pytkowicz, R.M., Suess, E. and Chen, C.T. (1992) The effect of magnesium-to-calcium ratios in artificial seawater, at different ionic products, upon the induction time, and the mineralogy of calcium carbonate: a laboratory study. *Geol. Rundsch*. **81/2**, 571-578

Sabbides, T.G. and Koutsoukos, P.G. (1993) The crystallization of calcium carbonate in artificial seawater; role of the substrate. *J. Cryst. Growth* **133**, 13-22

Sachez-Roman, M., Vasconcelos, C., Schmid, T., Dittrich, M, McKenzie, J.A., Zenobi, R. and Rivadeneyra, M.A. (2008) Aerobic microbial dolomite at the nanometer scale: Implications for the geologic record. *Geology* **36**, 879-882

Sachez-Roman, M., McKenzie, J.A., Wagener, A.L.R., Rivadeneyra, M.A. and Vasconcelos, C. (2009) Presence of sulfate does not inhibit low-temperature dolomite precipitation. *Earth Planet. Sci. Lett*. **285**, 131-139

Schmidt, M., Stumpf, T., Walther, C., Geckeis, H. and Fanghanel, T. (2010) Phase transformation in $CaCO_3$ polymorphs: A spectroscopic, microscopic and diffraction study. *J. Colloid Interface Sci.* **351**, 50-56

Shiraki, R. and Brantley, S.L. (1995) Kinetics of near-equilibrium calcite precipitation at 100°C: An evaluation of elementary-reaction based and affinity-based rate laws. *Geochim. Cosmochim. Acta* **58**, 1457–1471

Slaughter, M. and Hill, R.J. (1991) The influence of organic matter in organogenic dolomitization. *J. Sediment. Res*. **61**, 296-303

Söhnel, O. and Mullin, J.W. (1978) A method for the determination of precipitation induction periods. *J. Cryst. Growth* **44**, 377-382

Söhnel, O. and Mullin, J.W. (1982) Precipitation of calcium carbonate. *J. Cryst. Growth* **60**, 239-250

Soloviev, A., Ivanov, D., Tufeu, R. and Kanaev, A.V. (2001) Nanoparticle growth during the induction period of the sol-gel process. *J. Mater. Sci. Lett*. **20**, 905-906

Teng, H.H., Xu, H., Zhang, F. and Xu, J. (2012) Effect of water and sulfide on magnesium carbonate crystallization. In: Abstracts of the 22nd Annual V.M. Goldschmidt Conference, Montréal, Canada.

Titschack, J., Radtke, U. and Freiwald, A. (2009) Dating and characterization of polymorphic transformation of aragonite to calcite in Pleistocene bivalves from Rhodes (Greece) by combined shell microstructure, stable isotope, and electron spin resonance study. *J. Sediment. Res*. **79**, 332-346

Treccani, L., Mann, K., Heinemann, F. and Fritz, M. (2006) Perlwapin, an abalone nacre protein with three four-disulfide core (whey acidic protein) domains, inhibits the growth of calcium carbonate crystals. *Biophys. J.* **91**, 2601-2608

Vasconcelos, C. and McKenzie, J.A. (1997) Microbial mediation of modern dolomite precipitation and diagenesis under anoxic conditions (Lagoa Vermelha, Rio de Janeiro, Brazil). *J. Sediment. Res*. **67**, 378-390

Vasconcelos, C., McKenzie, J.A., Bernasconi, S., Grujic, D. and Tiens, A.J. (1995) Microbial mediation as a possible mechanism for natural dolomite formation at low temperatures. *Nature* **377**, 220–222

Waly, T., Kennedy, M.D., Witkamp, G., Amy, G. and Schippers, J.C. (2012) The role of inorganic ions in the calcium carbonate scaling of seawater reverse osmosis systems. *Desalination* **284**, 279-287

Wang, D., Wallace, A.F., De Yoreo, J.J. and Dove, P.M. (2009) Carboxylated molecules regulate magnesium content of amorphous calcium carbonates during calcification. *PNAS* **106**, 21511-21516

Warthmann, R., Lith, Y.V., Vasconcelos, C., McKenzie, J.A. and Karpoff, A.M. (2000). Bacterially induced dolomite precipitation in anoxic culture experiments. *Geology* **28**, 1091–1094

Wray, J.L. and Daniels, F. (1957) Precipitation of calcite and aragonite. *Am. Chem. Soc. J.* **79**, 2031-2034

Wright, D.T. and Wacey, D. (2004) Sedimentary dolomite – a reality check. In The Geometry and Petrogenesis of Dolomite Hydrocarbon Reservoirs

(Eds. C.J.R. Braithwaite, G. Rizzi and G. Darke), *Geological Society Special Publication* **235**, pp. 65–74.

Zhang, Y. and Dawe, R.A. (2000) Influence of Mg^{2+} on the kinetics of calcite precipitation and calcite crystal morphology. *Chem. Geol.* **163**, 129–138

Zhang, Y., Shaw, H., Farquhar, R. and Dawe, R. (2001) The kinetics of carbonate scaling-application for the prediction of downhole carbonate scaling. *J. Petroleum. Sci. Eng*. **29**, 85–95

Zhang, F., Konishi, H., Xu, H. and Roden, E.E. (2008) Mineralogical biosignature of high-magnesian calcite. In: American Geophysical Union. Abstract #P51A-1400

Zhang, F., Xu, H., Konishi, H., Shelobolina, E.S. and Roden, E.E. (2012) Polysaccharide-catalyzed nucleation and growth of disordered dolomite: A potential precursor of sedimentary dolomite. *Am. Mineral.* **97**, 556-567

Zuddas, P., Pachana, K. and Faivre, D. (2003) The influence of dissolved humic acids on the kinetics of calcite precipitation from seawater solutions. *Chem. Geol*. **201**, 91-101

Chapter 3 Final Remarks

3.1 Research Summary and Conclusions

Calcite ($CaCO_3(s)$) and dolomite ($CaMg(CO_3)_2(s)$) are by far the most abundant rock-forming carbonate minerals, comprising more than 90% of natural carbonates in the Earth's crust. The scarcity of modern dolomite contrasts strongly with its common abundance in ancient sedimentary rocks, leading to the paradox commonly referred to as the "dolomite problem", an issue that has puzzled scientist for over two centuries (e.g., Chilingar, 1956; Ronov, 1964). The relative abundance of ancient dolomite has been reported to correlate with periods of high sea-level stand and warm climatic conditions during which calcitic ooids and cements are common (Mackenzie and Morse, 1992; Arvidson and Mackenzie, 1996). Although it has been proposed that natural environments conducive to dolomite formation may be dynamic systems (Deelman, 1999, 2001; dos Anjos et al., 2011), in which the water chemistry (pH, alkalinity, saturation state with respect to specific mineral) may fluctuate, there is a scarcity of documented research dedicated to simulating such environmental changes. With this in mind, the objective of this research project was to investigate if alternating between episodes of dissolution and precipitation, by purging gases of different pCO_2 in natural seawater, would allow the water chemistry to fluctuate and simulate the dynamic nature of natural environments, possibly leading to dolomite formation. The seawater carbonate chemistry was monitored throughout the experiments and the saturation state with respect to carbonate minerals (e.g. aragonite, calcite and dolomite) was computed. The mineralogy of the initial, intermediate and final precipitates was determined by X-ray powder diffraction.

In the experiments carried out at 25 and 40°C, aragonite was obtained during the first few nucleation/precipitation cycles, but only calcite was detected in the 18th cycle of the experiments conducted at 25°C. We believe that through multiple cycles, calcite nuclei were formed and preserved at the expense of aragonite nuclei, providing enough seeds for growth during periods of supersaturation and thus breaking the Ostwald Step Rule. At 40°C, however, similar experiments always yielded aragonite. Although it has been reported that aragonite is more likely to form than calcite from seawater at higher temperatures (Morse and He, 1993), by alternating between periods of aragonite supersaturation and undersaturation, we expected to concentrate enough stable nuclei (i.e. calcite and dolomite) in solution. Given the shorter induction period of nucleation at 40°C (compared to 25°C), the more stable nuclei may not have accumulated to a high enough concentration after 25 cycles that a sufficient amount of calcite surfaces was available for growth to offset the nucleation of aragonite (Burton and Walter, 1987). Alternatively, it may be that the mineralogy of the precipitate is determined by the conformation and composition of stable pre-nucleation clusters that formed in the undersaturated solution (Gebauer et al., 2008). In turn, the nature of these pre-nucleation clusters may be determined by the solution composition and temperature.

3.2 Final Remarks and Recommendations

1) Natural seawater was used in this study to better simulate a dynamic natural system. Nevertheless, the composition of natural seawater is more complicated than artificial seawater and its use as a parent solution could have contributed to the longer induction periods and undesired results at 40°C. The presence of trace elements (e.g. Mn^{2+}, Fe^{2+}, Ba^{2+}) and dissolved organic compounds (e.g. soluble proteins, polysaccharides, humic acids) in natural seawater may catalyse or inhibit calcium carbonate nucleation (Mucci, 1988; Zuddas et al., 2003; Treccani et al., 2006; Nehrke et al., 2007; Lakshtanov et al., 2011; Waly et al., 2012; Zhang et al., 2012). For example, there are contrasting reports on the influence of polysaccharide on calcite nucleation. Whereas Giuffre et al. (2012) reported that polysaccharides can promote the formation of calcite, Yang et al. (2008) and Lakshtanov et al. (2011) observed the inhibition of calcite crystallisation by alginates, anionic polysaccharides. Given the discrepancy between experimental results and the poorly defined interactions between trace elements and dissolved organic compounds on carbonate crystallization, artificial seawater should be used in future studies of calcite/dolomite nucleation/precipitation to avoid the presence of these substances.

2) The pH(TRIS) values in our study varied between 6.4 and 8.0 during CO_2/N_2 and ambient air bubbling, respectively. In previous studies in which dolomite was successfully precipitated at low temperature, the pH values varied from approximately 7.0 to 9.0 (e.g. Oppenheimer and Master, 1965; Deelman, 1999; dos Anjos et al., 2011). This pH range is the same to those in which

dolomite formation was microbially-mediated (e.g. Sánchez-Román et al., 2008). The lower limit of their pH range (pH ≥ 7) was utilized to maximize the carbonate ion activities and overcome the hydration energy barrier of Mg^{2+} ions, whereas the upper limit of their pH range (pH ≤ 9) was set to avoid the concurrent precipitation of brucite ($Mg(OH)_2$) (Gebauer et al., 2008). Hence, future experiments should be conducted at a higher pH range (i.e. pH 7-9) to examine the potential for low-temperature dolomite precipitation.

3) Increasing the saturation state of a solution with respect to dolomite is commonly accepted as one of the effective factors to overcome the inhibition of dolomite precipitation (Compton, 1988). In ancient natural aquatic systems from which dolomite was precipitated, the supersaturation is thought to have been generated through CO_2 degassing during heating by sunlight and active CO_2 drawdown by photosynthesis (Arp et al., 2001). To simulate these processes, the natural seawater solution should have been heated between CO_2/N_2 bubbling and ambient-air bubbling. Because photosynthesis requires sunlight and can only occur during daytime, one would also expect the surface seawater temperature to increase during this period. Therefore, I suggest that during high pCO_2 bubbling, which simulates night-time respiration, the solution temperature could be held at 20°C, similar to the average ocean water temperature (17°C); whereas during ambient-air bubbling, simulating CO_2 drawdown by photosynthesis, the temperature could be raised to 25°C or higher to simulate heating by sunlight during day-time.

3.3 Current State of Knowledge and Future Avenues of Research

Parts of the objectives in this study—breaking the Ostwald step rule and synthesizing calcite from natural seawater at 25°C—were achieved. Nevertheless, the objective of precipitating dolomite at 25 and 40°C was not met. For numerous years, laboratory experiments have been conducted in an attempt to precipitate dolomite under near-surface conditions, i.e. at temperatures around 25°C and atmospheric pressure (e.g. Land, 1998; Chai et al., 1995; Warren, 2000), but few of them achieved their goal.

3.3.1 Experimental Conditions Leading to Low-Temperature Dolomite Precipitation

It has been proposed that dynamic natural systems or fluctuations in water chemistry are conducive to dolomite formation. In 1960s, Oppenheimer and Master (1965) successfully precipitated dolomite by modifying the pH and alkalinity of a seawater solution in order to simulate the influence of the daily photosynthetic cycle. In their experiment, they cultivated an algal mat collected in Florida on top of calcareous sand in artificial seawater (prepared according to the recipe of Lyman and Fleming, 1940). All aquaria were exposed to programmed artificial-light and dark periods of 24-hours. The pH varied from 7.4 (during the dark phases) to 9.2 (during illumination periods), and the total alkalinity changed from 1.7 mM/L during the periods of darkness to 2.5 mM/L during illumination phase. After 30 days, small amounts of dolomite were detected. Friedman and Foner (1982) duplicated these experiments with algal mats from the Red Sea, but, surprisingly, no diurnal pH fluctuations were observed and no carbonates were precipitated. They hypothesized that the much thicker algal mats they used throughout the experiment may have generated H_2S, buffering pH changes in the waters.

Deelman (1999) made several attempts at precipitation low-temperature dolomite. Rather than simulating the natural daily photosynthetic cycle by switching artificial light on and off, he alternatively bubbled and stripped CO_2 from an artificial seawater solution. The working hypothesis being that multiple alternating cycles of precipitation and dissolution would lead to the accumulation of more stable phases at the expense of metastable phases. The artificial seawater was made up of the following reagent grade chemicals: 53.71 g NaCl; 6.43 g $MgCl_2.6H_2O$; 4.48 g $MgSO_4.7H_2O$; 1.52 g KCl; 1.00 g urea and 0.20 g $CaCO_3$. All salts were dissolved in 330 ml of distilled water. After complete dissolution, calcium carbonate and urea were added. The addition of urea was found to favour the low-temperature nucleation of dolomite, and the catalysis was deemed to be related to the desorption of chloride ions from calcium carbonate surfaces (Deelman, 1999). After 14 cycles of alternating between episodes of dissolution and precipitation (each cycle consists of 12 hours of CO_2 bubbling and 60 hours of CO_2 stripping), dolomite was formed. One study aimed at duplicating Deelman's results was recently carried out by dos Anjos et al. (2011), but only magnesite was obtained. The different results might be due to the experimental temperature, which was 5°C higher in the study of dos Anjos et al (2011).

Although using different experimental protocols, the objective of both the Oppenheimer and Master (1965) and Deelman (1999) approaches was to simulate fluctuations of natural systems in order to precipitate dolomite at low temperature. The worthiness of these protocols deserves further investigation.

3.3.2 The Mechanisms of Microbially-Mediated Dolomitization

An association between micro-organisms and carbonate precipitation has long been recognized both in modern and ancient sedimentary environments, as well as in laboratory studies (Buczynski and Chafetz, 1991; Wright and Oren, 2005; Kenward et al., 2009).

Several mechanisms have been proposed to explain the role(s) of organic compounds and microbes in promoting dolomitization. For example, it has been suggested that the metabolism of sulfate-reducing bacteria (SRB) and methanogens can increase the alkalinity and pH of the host environments, enhancing the desolvation of Mg^{2+} ions, and promoting dolomite formation (Kenward et al., 2009). Nevertheless, the mechanism by which SRB metabolism promotes dolomite formation is highly debated. Many authors claimed that SRB can mediate dolomite formation by the removal of dissolved sulfate, which is a potential dolomite precipitation inhibitor (Vasconcelos et al., 1995; Vasconcelos and McKenzie, 1997; Warthmann et al., 2000; Van Lith et al. 2003; Wright and Wacey, 2005); whereas others suggested that the presence of sulfide, produced by SRB, serves as a catalyst for Mg-rich carbonate mineral and dolomite formation (Teng et al., 2012; Zhang et al., 2008). One or both of these mechanisms may provide the key(s) to the dolomite problem and, thus, warrant further investigations.

Recently, the promotion of dolomite nucleation and growth by extracellular polymeric substances (EPS) and dissolved polysaccharides secreted by organisms has been proposed by Bontognali et al. (2007, 2008), and further investigated by other researchers (Krause et al., 2012; Xu, 2012; Zhang et al., 2012). EPS is a broad term that encompasses a variety of organic polymers secreted by microbial cells in the environment. Polysaccharides are the major component of most EPS, commonly in combination with polypeptides, nucleic acids, phospholipids, and other polymeric compounds (Decho, 1990). The most widely accepted explanation is that the carboxylic functional groups of the EPS and dissolved polysaccharides may complex Mg^{2+} and weaken the hydration sphere of Mg^{2+} ions on growing Ca-Mg carbonate surfaces, and, thus, enhance Mg^{2+} incorporation into the carbonate (Zhang et al., 2012; Xu, 2012). Conversely, Hamm et al. (2010) proposed that carboxylate groups may promote dehydration of Ca^{2+}, but do not affect the solvation sphere of Mg^{2+}. More work is needed to resolve these apparently contradictory interpretations. Moreover, some authors proposed that polysaccharides may inhibit calcite crystallization by blocking calcite active growth sites (Yang et al., 2008; Lakshtanov et al., 2011). If this statement is true, the formation of dolomite could also be explained by kinetics--by inhibiting the simpler structured minerals (i.e. calcite), enough time would be allowed for highly ordered mineral (i.e. dolomite) to be precipitated. Despite some progress in explaining the role(s) of specific organic compounds and microbes in dolomitization, the mechanism is still poorly constrained and further research is needed to elucidate the mechanism.

3.4 Future Research

To summarize the above, future research to investigate the mechanism of marine dolomite precipitation should be conducted in artificial seawater in the presence of micro-organisms (e.g. SRB), their metabolites (e.g. polysaccharides) or specific functional groups (e.g. carboxyl). The solution pH range should be varied between 7 and 9, and the experimental temperature allowed to fluctuate around 25^oC and lower than atmospheric pCO_2 to simulate the daily photosynthetic cycle and well beyond 25^oC and $S = 35$ given that the very early (fabric retentive) dolomite, that characterizes much of the carbonate record, likely formed in shallow to supratidal environments in hot and arid zones (Illing et al., 1965; Warren, 2000).

3.5 Implications

The chemical composition of abiotic and biogenic marine carbonate minerals has been extensively used as a tool to elucidate historic changes in the Earth's ocean chemistry (Hardie, 1996; Lopez et al., 2009). Today, high-Mg calcite and aragonite are dominantly associated with warm tropical to subtropical waters whereas, in the past, they were abundant under cooler climatic conditions (Lopez et al., 2009). Conversely, low-Mg calcites are generally found at higher latitudes or in cool deep waters of the modern ocean whereas, in the past, they were mainly associated with warmer global climatic periods (Wilkinson and Algeo, 1989; Lopez et al., 2009). Experimental investigations have shown that the Mg content of abiotic calcite samples is positively correlated with temperature (Mucci, 1987; Arvidson and Mackenzie, 2000), consistent with the latitudinal distribution of present-day of the Mg content of abiotic marine calcites, but in contrast with interpretations of past climate records. This apparent discrepancy may be attributable to variations of the $[Mg^{2+}]:[Ca^{2+}]$ ratio in ancient oceans and/or major changes in the saturation state of the ocean water (Lopez et al., 2009). The relative abundance of $CaCO_3$ minerals, specifically the calcite: aragonite ratio, in marine sediments has been proposed as an indicator of paleo-seawater $[Mg^{2+}]:[Ca^{2+}]$ ratio (Hardie, 1996). On the other hand, in our study, by solely varying the pCO_2 with minor/negligible variations in seawater $[Mg^{2+}]:[Ca^{2+}]$ ratio at a constant temperature, the mineralogy of the precipitate was modified at 25°C. Variations in paleo-atmospheric pCO_2 can modify the saturation state of near-surface seawater as the CO_2 exchange across the air-sea interface is rapid (~3 months; Broecker and Peng, 1982). Hence, carbonate mineralogy may be a potential proxy of climate, ocean chemistry ($[Mg^{2+}]:[Ca^{2+}]$ ratio) and atmospheric pCO_2 through geological time.

3.6 References

Arp, G., Reimer, A. and Reitner, J. (2001) Photosynthesis-induced biofilm calcification and calcium concentrations in Phanerozoic oceans. *Science* **292**, 1701-1704

Arvidson, R.S. and Mackenzie, F.T. (1996) Tentative kinetic model for dolomite precipitation rate and its application to dolomite distribution. *Aquat. Geochem*. **2**, 273-298

Arvidson, R.S. and Mackenzie, F.T. (2000) Temperature dependence of mineral precipitation rates along the $CaCO_3$-$MgCO_3$ join. *Aquat. Geochem.* **6**, 249–256

Bontognali, T., Vasconcelos, C., Warthmann, R., Dupraz, C. and McKenzie, J.A. (2007) The role of extracellular polymeric substances in the nucleation of microbial dolomite. In: 17th Annual V.M. Goldschmidt Conference, Cologne, Germany. pp A108-A108

Bontognali, T., Vasconcelos, C., Warthmann, R., Dupraz, C., Bernasconi, S.M. and McKenzie, J.A. (2008) Microbes produce nanobacteria-like structures, avoiding cell entombment. *Geology* **36**, 663-666

Broecker, W.S. and Peng, T. (1982) Tracers in the Sea. Lamont-Doherty Earth Observatory, Palisades, N.Y. pp.690.

Buczynski, C. and Chafetz, H.S. (1991) Habit of bacterially induced precipitates of calcium carbonate and the influence of medium viscosity on mineralogy. *J. Sediment. Res.* **61**, 226–233

Burton, E.A. and Walter, L.M. (1987) Relative precipitation rates of aragonite and Mg calcite from seawater: Temperature or carbonate ion control? *Geology* **15**, 111-114

Chai, L., Navrotsky, A. and Reeder, R.J. (1995) Energetics of calcium-rich dolomite. *Geochim. Cosmochim. Acta* **5**, 939-944

Chilingar, G.V. (1956) Relationship between Ca/Mg ratio and geological age. *Bull. Am. Ass. Petrol. Geol.* **40**, 2256-2266

Compton, J.S. (1988) Degree of supersaturation and precipitation of organogenic dolomite. *Geology* **16**, 318-321

Decho, A.W. (1990) Microbial exopolymer secretions in ocean environments: Their role(s) in food webs and marine processes. *Oceanography and Marine Biology Annual Review* **28**, 73–153

Deelman, J.C. (1999) Low-temperature nucleation of magnesite and dolomite. *N. Jb. Miner. Mh*. **7**, 289-302

Deelman, J.C. (2001) Breaking Ostwald's rule. *Chem. Erde* **61,** 224-235

dos Anjos, A.P.A., Sifeddine, A., Sanders, C.J. and Patchineelam, S.R. (2011) Synthesis of magnesite at low temperature. *Carbonates and Evaporites* **26**, 213-215

Friedman, G.M. and Foner, H.A. (1982) pH and Eh changes in sea-marginal algal pools of the red sea: and their effect on carbonate precipitation. *J. Sediment. Petrol.***52**, 41-46

Gebauer, D., Völkel, A. and Cölfen, H. (2008) Stable prenucleation calcium carbonate clusters. *Science* **322**, 1819-1822

Giuffre, A.J., Hamm, L.M. and Dove, P.M. (2012) Controls of polysaccharide chemistry on kinetics and thermodynamics of calcium carbonate nucleation. In: Abstracts of the 22nd Annual V.M. Goldschmidt Conference, Montréal, Canada.

Hamm, L.M., Wallace, A.F. and Dove, P.M. (2010) Molecular dynamics of ion hydration in the presence of small carboxylated molecules and implications for calcification. *J. Phys. Chem. B* **114**, 10488-10495

Hardie, L.A. (1996) Secular variation in seawater chemistry: An explanation for the coupled secular variation in the mineralogies of marine limestones and potash evaporites over the past 600 m.y. *Geology* **24**, 279-283

Illing, L.V., Wells, A.J. and Taylor, J.C.M. (1965) Penecontemporaneous dolomite in the Persian Gulf. In: Dolomitization and Limestone Diagenesis (Eds., L.C. Pray and R.C. Murray). *Soc. Econ. Paleont. Miner.* **13**, pp. 89–111.

Kenward, P.A., Goldstein, R.H., Gonzalez, L.A. and Roberts, J.A. (2009) Precipitation of low-temperature dolomite from an anaerobic microbial consortium: the role of methanogenic Archaea. *Geobiology* **7**, 556–565

Krause, S., Liebetrau, V., Gorb, S., Sánchez-Román, M., McKenzie, J.A. and Treude, T. (2012) Microbial nucleation of Mg-rich dolomite in exopolymeric substances under anoxic modern seawater salinity: New insight into an old enigma. *Geology* **40**, 587-590

Lakshtanov, L.Z., Bovet, N. and Stipp, S.L.S. (2011) Inhibition of calcite growth by alginate. *Geochim. Cosmochim. Acta* **75**, 3945-3955

Land, L.S. (1998) Failure to precipitate dolomite at 25^{o}C from dilute solution despite 1000-fold oversaturation after 32 years. *Aquat. Geochem.* **4**, 361-368

Lopez, O., Zuddas, P. and Faivre, D. (2009) The influence of temperature and seawater composition on calcite crystal growth mechanisms and kinetics: Implications for Mg incorporation in calcite lattice. *Geochim. Cosmochim. Acta* **73**, 337-347

Lyman, J. and Fleming, R.H. (1940) Composition of sea water. *J. Mar. Res*. **3**, 134-146

Mackenzie, F.T. and Morse, J.W. (1992) Sedimentary carbonates through Phanerozoic time. *Geochim. Cosmochim. Acta* **56**, 3281-3295

Morse, J.W. and He, S. (1993) Influences of T, S and PCO_2 on the pseudo-homogeneous precipitation of $CaCO_3$ from seawater: implications for whiting formation. *Mar. Chem*. **41**, 291-297

Mucci, A. (1987) Influence of temperature on the composition of magnesian calcite overgrowths precipitated from seawater. *Geochim. Cosmochim. Acta* **51**, 1977–1984

Mucci, A. (1988) Manganese uptake during calcite precipitation from seawater: Conditions leading to the formation of a pseudokutnahorite. *Geochim. Cosmochim. Acta* **52**, 1859-1868

Nehrke, G., Reichart, G.J., Van Cappellen, P., Meile, C. and Bijma, J. (2007) Dependence of calcite growth rate and Sr partitioning on solution stoichiometry: non-kossel crystal growth. *Geochim. Cosmochim. Acta* **71**, 2240-2249

Oppenheimer, C.H. and Master, M. (1965) On the solution of quartz and precipitation of dolomite in sea water during photosynthesis and respiration. *Zeitsch. Allg. Midrobiologie* **5**, 48-51

Ronov, A.B. (1964) Common tendencies in the chemical evolution of the Earth's crust, ocean and atmosphere. *Geochem. Int*. **4**, 713-737

Sánchez-Román, M., Vasconcelos, C., Schmid, T., Dittrich, M., McKenzie, J.A., Zenobi, R. and Rivadeneyra, M.A. (2008) Aerobic microbial dolomite at the nanometer scale: Implications for the geologic record. *Geology* **36**, 879–882

Teng, H.H., Xu, H., Zhang, F. and Xu, J. (2012) Effect of water and sulfide on magnesium carbonate crystallization. In: Abstracts of the 22nd Annual V. M. Goldschmidt Conference, Montréal, Canada.

Treccani, L., Mann, K., Heinemann, F. and Fritz, M. (2006) Perlwapin, an abalone nacre protein with three four-disulfide core (whey acidic protein) domains, inhibits the growth of calcium carbonate crystals. *Biophys. J.* **91**, 2601-2608

Van Lith, Y., Warthmann, R., Vasconcelos, C. and McKenzie, J.A. (2003) Microbial fossilization in carbonate sediments: a result of the bacterial surface involvement in dolomite precipitation. *Sedimentology* **50**, 237–245

Vasconcelos, C. and McKenzie, J.A. (1997) Microbial mediation of modern dolomite precipitation and diagenesis under anoxic conditions (Lagoa Vermelha, Rio de Janeiro, Brazil). *J. Sediment. Res.* **67**, 378–390

Vasconcelos, C., McKenzie, J.A., Bernasconi, S., Grujic, D. and Tien, A.J. (1995) Microbial mediation as a possible mechanism for natural dolomite formation at low-temperatures. *Nature* **377**, 220–222

Waly, T., Kennedy, M.D., Witkamp, G., Amy, G. and Schippers, J.C. (2012) The role of inorganic ions in the calcium carbonate scaling of seawater reverse osmosis systems. *Desalination* **284**, 279-287

Warthmann, R., van Lith, Y., Vasconcelos, C., McKenzie, J.A. and Karpoff, A.M. (2000) Bacterially induced dolomite precipitation in anoxic culture experiments. *Geology* **28**, 1091–1094

Warren, J (2000) Dolomite: occurrence, evolution and economically important associations. *Earth Sci. Rev.* **52**, 1–81

Wilkinson, B.H. and Algeo, T.J. (1989) Sedimentary carbonate record of calcium-magnesium cycling. *Am. J. Sci.* **289**, 1158-1194

Wright, D.T. and Oren, A. (2005) Nonphotosynthetic bacteria and the formation of carbonates and evaporites through time. *Geomicrobiol. J.* **22**, 27–53

Wright, D.T. and Wacey, D. (2005) Precipitation of dolomite using sulphate-reducing bacteria from the Coorong Region, South Australia: significance and implications. *Sedimentology* **52**, 987–1008

Xu, H. (2012) Sweet spot for the formation of sedimentary dolomite. In: Abstracts of the 22nd Annual V.M. Goldschmidt Conference, Montréal, Canada.

Yang, M., Stipp, S.L.S. and Harding, J. (2008) Biological control on calcite crystallization by polysaccharides. *Cryst. Growth Design* **8**, 4066-4074

Zhang, F., Konishi, H., Xu, H. and Roden, E.E. (2008) Mineralogical biosignature of high-magnesian calcite. In: American Geophysical Union. Abstract #P51A-1400

Zhang, F., Xu, H., Konishi, H., Shelobolina, E.S. and Roden, E.E. (2012) Polysaccharide-catalyzed nucleation and growth of disordered dolomite: A potential precursor of sedimentary dolomite. *Am. Mineral.* **97**, 556-567

Zuddas, P., Pachana, K. and Faivre, D. (2003) The influence of dissolved humic acids on the kinetics of calcite precipitation from seawater solutions. *Chem. Geol*. **201**, 91-101